Seewald, Jeffrey S. ; Reeves, Eoghan P. ; Bach, Wolfgang ; Saccocia, Peter J. ; Craddock, Paul R. ; Walsh, Emily ; Shanks, Wayne C. ; Sylva, Sean P. ; Pichler, Thomas ; Rosner, Martin

Geochemistry of hot-springs at the SuSu Knolls hydrothermal field, Eastern Manus Basin: Advanced argillic alteration and vent fluid acidity

Journal Article as: peer-reviewed accepted version (Postprint)

DOI of this document*(secondary publication): https://doi.org/10.26092/elib/3155

Publication date of this document: 01/08/2024

* for better findability or for reliable citation

Recommended Citation (primary publication/Version of Record) incl. DOI:

Seewald, Jeffrey S. ; Reeves, Eoghan P. ; Bach, Wolfgang ; Saccocia, Peter J. ; Craddock, Paul R. ; Walsh, Emily ; Shanks, Wayne C. ; Sylva, Sean P. ; Pichler, Thomas ; Rosner, Martin. 2019. Geochemistry of hot-springs at the SuSu Knolls hydrothermal field, Eastern Manus Basin: Advanced argillic alteration and vent fluid acidity. In: Geochimica et Cosmochimica Acta, vol. 255, pp. 25-48. © Elsevier. DOI: 10.1016/j.gca.2019.03.034.

Geochemistry of hot-springs at the SuSu Knolls hydrothermal field, Eastern Manus Basin: Advanced argillic alteration and vent fluid acidity

Jeffrey S. Seewald[a,*], Eoghan P. Reeves[a,1], Wolfgang Bach[b], Peter J. Saccocia[c], Paul R. Craddock[a,2], Emily Walsh[c], Wayne C. Shanks III[d], Sean P. Sylva[a], Thomas Pichler[b], Martin Rosner[e]

[a] *Department of Marine Chemistry and Geochemistry, Woods Hole Oceanographic Institution, 360 Woods Hole Road, Woods Hole, MA 02543, USA*
[b] *Geoscience Department, University of Bremen, Klagenfurter Str., 28359 Bremen, Germany*
[c] *Department of Geological Sciences, Bridgewater State University, Bridgewater, MA 02325, USA*
[d] *U.S. Geological Survey, 973 Denver Federal Center, Denver, CO 80225, USA*
[e] *Freie Universität Berlin, Institut für Geologische Wissenschaften, Malteserstrasse 74-100, 12249 Berlin, Germany*

Keywords: Back-arc basin; Hydrothermal systems; Magmatic volatiles; Fluid-rock interaction; Acid-sulfate fluids; Manus Basin; SuSu; Knolls

---

[*] Corresponding author.
E-mail address: jseewald@whoi.edu (J.S. Seewald).

[1] Present address: Department of Earth Science and K.G. Jebsen Centre for Deep Sea Research, University of Bergen, Bergen N-5020, Norway.

[2] Present address: Schlumberger-Doll Research Center, Cambridge, MA 02139, USA.

1. INTRODUCTION

Hydrothermal fluids in back-arc environments are characterized by a broad range of compositions that reflect substantial variability in chemical and physical conditions during fluid rock interaction within the oceanic lithosphere (Fouquet et al., 1993; Ishibashi et al., 1996; Gamo et al., 1997; Takai et al., 2008; Mottl et al., 2011; Reeves et al., 2011; Kawagucci et al., 2013; Seewald et al., 2015). A significant portion of this variability can be attributed to deep-seated processes involving the influence of the subducted slab on the composition of lithospheric rocks and shallow magmas. Water-rich fluids that can exsolve from crystallizing magmas at shallow levels in the crust can play a fundamental role in regulating the composition of back-arc hydrothermal fluids because they may represent a direct source of metals and/or acidity (Hedenquist and Lowenstern, 1994; Yang and Scott, 1996, 2002, 2006). Relative to magmatic volatiles entrained in mid-ocean ridge hydrothermal fluids that are dominated by CO_2, magmatic volatiles in back-arc environments may be substantially more acidic due to high levels of SO_2, HCl, and HF in addition to CO_2 and H_2O. The presence of SO_2 is particularly significant because its disproportionation upon cooling and mixing rapidly produces sulfuric acid (H_2SO_4). Unlike CO_2 which is a relatively weak acid, especially at elevated temperatures, H_2SO_4 and HCl are stronger acids that can significantly decrease the pH of hydrothermal fluids venting at the seafloor. Because fluid-mineral interaction during the transport of hydrothermal fluids in subsurface environments is strongly dependent on pH, highly acidic magmatic volatiles will influence the alteration of the back-arc oceanic lithosphere and the aqueous mobility of sulfide forming metals.

Two distinct styles of hydrothermal venting have been documented in back-arc environments (Fig. 1; de Ronde and Stucker, 2015; Seewald et al., 2015). One is broadly similar to hydrothermal circulation at mid-ocean ridges and involves the convective circulation of seawater-derived hydrothermal fluids through the lithosphere where fluid-rock interaction and magmatic degassing modifies the chemistry of seawater to produce acidic, reducing, and metal-rich fluids that vent at the seafloor (Fouquet et al., 1993; Takai et al., 2008; Mottl et al., 2011; Reeves et al., 2011). When hydrothermal fluids are transition metal-rich, mixing with seawater upon venting to the water column induces rapid precipitation of minerals and the formation of 'smoker-type' vent fluids that form massive sulfide deposits.

The second style of venting involves the direct degassing of magmatic volatiles from a magma chamber/intrusion. The volatiles mix with unmodified seawater in subsurface environments and are subsequently released at the seafloor (Gamo et al., 1997; Butterfield et al., 2011; Seewald et al., 2015). The fluids are often referred to as 'acid-sulfate' fluids owing to substantially higher levels of acidity relative to smoker fluids and large enrichments in aqueous ΣSO_4 ($\Sigma SO_4 = H_2SO_4 + HSO_4^- + SO_4^{2-}$). In contrast to processes responsible for the formation of smoker fluids, venting of acid-sulfate fluids does not appear to involve convective circulation of seawater (Seewald et al., 2015) and is analogous to sub-aerial fumarolic discharge. Acid-sulfate hot-springs typically contain high concentrations of elemental sulfur that results in the venting of milky white fluids at the seafloor.

The influence of magmatic degassing in back-arc environments extends beyond the direct contribution of magmatically-derived fluids to the chemistry of circulating smoker fluids or direct emanation into the water column. Volcanic host rocks at and below the seafloor have are extensively altered by acid-sulfate fluids producing a mineral assemblage containing quartz-illite-pyrophyllite-anhydrite ± alunite (Gena et al., 2001; Roberts et al., 2003; Lackschewitz et al., 2004) that is compositionally distinct from assemblages observed in mid-ocean ridge settings (e.g. Alt, 1995). Temporal changes in subsurface hydrology and the extent of magmatic volatile degassing may result in later interaction of these assemblages with less acidic seawater-derived hydrothermal fluids that contain relatively low levels of acidic magmatic volatiles. Although the effects of magmatic volatiles on hydrothermal fluid chemistry are now better understood (Gamo et al., 1997; Reeves et al., 2011; Butterfield et al., 2011; Seewald et al., 2015), the interactions of pre-existing acid-sulfate mineral assemblages with less acidic smoker-type fluids are not, but could have a profound effect on fluid composition.

Field study of hydrothermal activity at SuSu Knolls in 2006 revealed an area of ongoing magmatic activity and recent volcanism located in the back-arc environment of the Manus Basin in the Bismarck Sea, Papua New Guinea (Fig. 2). Hydrothermal activity at SuSu Knolls is associated with three adjacent neovolcanic domes known as Suzette, North Su, and South Su. Suzette, the northernmost edifice, hosts an active hydrothermal field along with a deposit of sulfide mineralization ("Solwara 1") that is the subject of commercial mining interest (Boschen et al., 2013). In 2006, fumarolic venting of magmatically-derived acid-sulfate fluids on the flanks of the North Su dome was observed within a few hundred meters of smoker-type vent fluids (Seewald et al., 2015; Thal et al., 2016). The close proximity of these two styles of hydrothermal venting provides a rare opportunity to assess the influence of magmatic volatiles and previously formed acid-sulfate mineral assemblages on the composition of smoker fluids formed by the convective circulation of seawater.

Here we report data for the chemical and isotopic composition of smoker-type hydrothermal fluids collected contemporaneously in 2006 with previously reported acid-sulfate fluids (Seewald et al. 2015) from the SuSu Knolls vent field during R/V *Melville* cruise MGLN06MV. Magmatic volatiles that may be involved with the formation of smoker fluids at North Su are likely derived from the same source as the magmatic volatiles responsible for the formation of nearby acid-sulfate vent fluids. Because the compositions of the magmatic volatiles have been determined by direct sampling of the North Su acid-sulfate fluids (Seewald et al., 2015), the contribution of magmatic volatiles to the chemistry of smoker fluids prior to mixing and

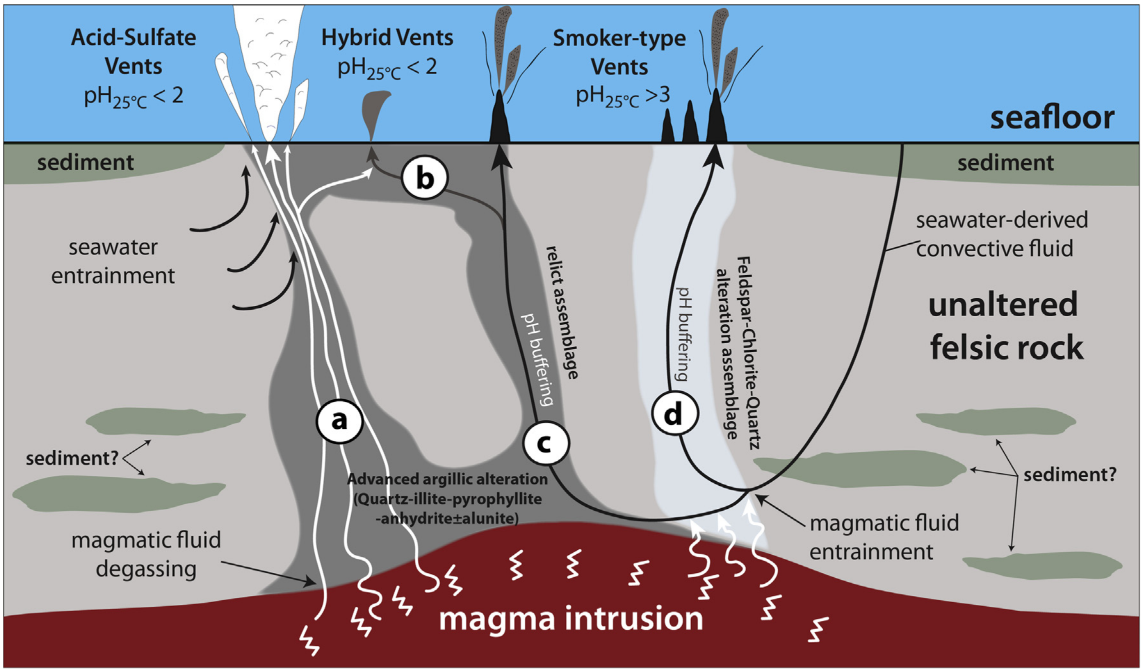

Fig. 1. Schematic representation of conceptual models for fluid-rock interaction processes that regulate the pH of hydrothermal fluids at the SuSu Knolls vent field. Degassing of highly acidic magmatic volatiles (white arrows) produces advanced argillic alteration assemblages in upflow zones. Venting of acid-sulfate fluids with pH$_{25^\circ C}$ values less than 1 (denoted by (a)) occurs when magmatic fluids reach the seafloor without being entrained by seawater-derived smoker fluids that are driven by hydrothermal convection (see Seewald et al., 2015). Hybrid vents with pH$_{25^\circ C}$ values less than 1 (denoted by (b)) reflect the mixing of magmatic volatiles with seawater-derived convective smoker fluids (black arrows) in the shallow subsurface just prior to venting. When seawater-derived smoker type fluids encounter regions of advanced argillic alteration formed by prior episodes of magmatic degassing (denoted by (c)), fluid pH$_{25^\circ C}$ is buffered by the relict mineral assemblage to values between 2 and 3 (e.g. vents NS4 and SZ5 in the present study). Interaction of seawater-derived convective fluids with crustal rocks that have not been previously altered by acid-sulfate fluids produces an assemblage containing feldspar-chlorite-quartz that buffers pH$_{25^\circ C}$ between values of 3 and 4 (denoted by (d)).

subsequent fluid-rock interaction can be constrained. Compositional information presented here is used in conjunction with geochemical models to reconstruct processes responsible for the formation and evolution of smoker fluids in a back-arc environment. Our results suggest that acidity of many smoker-type fluids may be regulated by equilibration with minerals formed during earlier periods of acid-sulfate alteration in hydrothermal upflow zones.

2. GEOLOGIC SETTING

The Manus Basin (Fig. 2), located in the northeastern Bismarck Sea, is a young (ca. 3.5 Ma) back-arc basin that is opening rapidly at full rates up to 137 mm/y (Tregoning, 2002). It is bordered to the north by the inactive Manus Trench and to the south by the active New Britain Trench (Taylor, 1979; Taylor et al., 1994; Lee and Ruellan, 2006). Volcanism associated with basin extension occurs along a series of spreading centers and rifts between the Willaumez, Djual, and Weitin transform faults (Taylor, 1979; Taylor et al., 1994; Martinez and Taylor, 1996). Fully-developed spreading in the center of the basin occurs along the 120 km-long Manus Spreading Center, which hosts the unsedimented Vienna Woods hydrothermal field in predominantly MORB-like crust (Both et al., 1986; Tufar, 1990; Lisitsyn et al., 1993; Reeves et al., 2011). In contrast, the Eastern Manus Basin, located between the Djaul and Weitin transform faults (Fig. 2), is an extensional transform zone within much older Eocene-Oligocene island-arc crust that likely formed during previous southwestward subduction along the Manus Trench (Binns and Scott, 1993; Binns et al., 2007). Volcanism associated with the incipient rifting of the pre-existing intermediate/felsic crust has produced a complex series of *en echelon* neovolcanic seafloor ridges and domes collectively known as the Eastern Manus volcanic zone (Fig. 2). Volcanic rocks in the Eastern Manus Volcanic Zone vary from basalt to rhyodacite (Binns and Scott, 1993; Kamenetsky et al., 2001; Sinton et al., 2003) and possess isotopic and major and trace element characteristics that resemble subaerial volcanoes of the New Britain Arc, indicating strong arc affinities (Sinton et al., 2003; Pearce and Stern, 2006).

During the last three decades, several areas of hydrothermal activity have been discovered in the Eastern Manus volcanic zone (Fig. 2), including the DESMOS caldera, the SuSu Knolls area, and the PACMANUS and

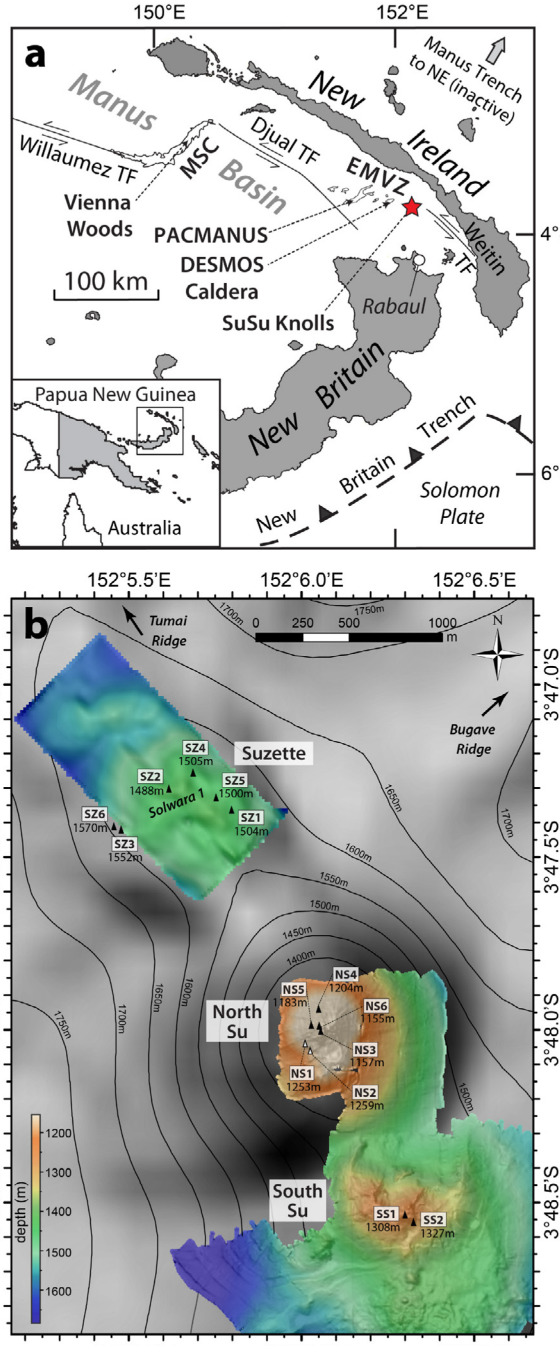

Fig. 2. (a) Regional map showing part of the Bismarck Archipelago (Papua New Guinea), Manus Basin, and the locations of the Manus Spreading Center (MSC), Eastern Manus Volcanic Zone (EMVZ), and major transform faults (TF), and (b) SM2000 bathymetric map of the SuSu Knolls hydrothermal field in 2006, underlain by SeaBeam bathymetry, showing the Suzette, North Su and South Su areas of hydrothermal venting (adapted from Tivey et al., 2006). Sampled smoker-type vents are denoted by solid triangles, with open triangles denoting the 2006 acid-sulfate fluids reported in Seewald et al. (2015). Note that substantial eruptive changes to topography occurred in this area immediately southwest of the North Su dome after 2006 (Thal et al. 2016).

Northeast Pual sites located on Pual Ridge (Binns and Scott, 1993; Gamo et al., 1993, 1997, 2006; Auzende et al., 1997, 2000; Binns et al., 1997; Gena et al., 2001, 2006; Moss and Scott, 2001; Tivey et al., 2006; Hrischeva et al., 2007; Craddock et al., 2010; Reeves et al., 2011; Seewald et al., 2015; Thal et al., 2014, 2016).

The hydrothermally-active neovolcanic edifices that constitute Suzette, North Su and South Su (Fig. 2) overlie the andesitic Tumai Ridge at water depths between 1150 and 1570 m (Binns et al., 1997; Auzende et al., 2000; Moss and Scott, 2001; Tivey et al., 2006; Hrischeva et al., 2007; Seewald et al., 2015). The North Su and South Su volcanic structures are composed of abundant porphyritic andesite to dacite flows showing variable advanced argillic alteration (i.e., quartz–pyrophyllite–illite ± alunite and native sulfur) by acid-sulfate fluids (Binns et al., 1997; Yeats et al., 2014; Tivey et al., 2006). The entire series of SuSu Knolls edifices is covered with a sediment apron of variable thickness up to several meters, consisting of layered, dark, and locally sulfidic sandy sediment that is most likely a mixture of volcanoclastic and pelagic/hemipelagic detritus (Hrischeva et al., 2007; Yeats et al., 2014).

The summit of the Suzette hydrothermal field (Fig. 2) is characterized by large expanses of both relict and scattered active sulfide chimneys that, in many instances, are buried within thick sediment. Hydrothermal activity is distributed over broad sections of the Suzette mound. Five vent fluids with temperatures from 226–303 °C were sampled from sulfide-rich chimney edifices. A sixth fluid (SZ5) with a temperature of 249 °C was sampled from a cracked pavement-like sulfide structure.

Hydrothermal fluids with temperatures varying from 299–325 °C were collected at the summit of the North Su dome from three separate massive sulfide structures up to 11 m tall within a large complex of smoker chimneys. An additional smoker-type fluid (NS4), which was grayer in appearance and had a temperature of 241 °C, was collected on the northwest flank of the dome. The North Su dome flanks also hosted numerous areas venting sulfur-rich milky white fluids with temperatures of 48–215 °C from talus piles consisting of extensively altered volcanic clasts and, in some cases, from areas with minor hydrothermal sediment cover (Seewald et al., 2015). Flows and flanges of native sulfur were common in the vicinity of the white fluids. In areas of more substantial hydrothermal sediment cover on the dome flanks, molten sulfur at temperatures of 272–284 °C was observed less than 0.5 m beneath the sediment-water interface. Several large lava spines protruded up to 15 m from the hydrothermal detritus, with diffuse fluid venting observed at their base. It has been suggested the lava spines reflect the gradual extrusion of highly viscous, crystal-rich andesitic magma into water-saturated, clast-dominated sediments on the slopes of the dome (Thal et al., 2016).

Hydrothermal activity at South Su was more limited. High-temperature fluids with maximum temperatures of 271 and 288 °C were collected from two chimneys that lacked discrete orifices, but instead emitted fluid diffusely at the top through highly porous material.

3. METHODS

Vent fluids were collected using isobaric gas-tight fluid samplers (Seewald et al., 2002) and syringe style ‘major’ samplers (Von Damm et al., 1985a) deployed from the ROV *Jason II.* Typically, two separate samples were collected from each vent using the gas-tight samplers (IGT-prefix in Table S1) and in most cases a third sample was collected using the ‘major’ sampler (M-prefix in Table S1). Vent fluid temperature was monitored continuously during fluid sampling using a thermocouple attached to the end of the sampler inlet snorkel. The reported temperatures (Table 1) represent maximum values recorded for each vent with an estimated uncertainty of ±2 °C.

Fluid samples were processed within 24 h of recovery on the ship. Shipboard analyses included pH measured at room temperature ($pH_{25°C}$) using a Ag/AgCl combination reference electrode, dissolved H_2 and CH_4 by gas chromatography with thermal conductivity detection following headspace extraction, and total aqueous sulfide ($\Sigma H_2S = H_2S + HS^- + S^{2-}$) following aqueous precipitation as Ag_2S for subsequent gravimetric determination in a shore-based laboratory. For each sample, several aliquots were stored in acid-cleaned high-density polyethylene bottles for shore-based analysis. Anions (Cl, ΣSO_4, Br, F) and cations (Na, K, Ca, Mg) were analyzed by ion chromatography. An aliquot of fluid was acidified with analytical-grade Optima® HCl prior to storage for trace metal analysis by inductively-coupled plasma mass spectrometry (ICP-MS) and inductively-coupled plasma atomic emission spectroscopy (ICP-AES). A sub-sample of the acidified aliquot was diluted 100-fold at sea for measurement of aqueous SiO_2 by ICP-AES. Samples of high temperature vent fluids typically contain transition metal-rich precipitates due to cooling and mixing with alkaline seawater during sampling. These precipitates were collected on 0.22 μm nylon filters and analyzed by ICP-MS after dissolution, allowing reconstruction of fluid composition prior to metal precipitation. Several aliquots of fluid were stored in 30 mL serum vials with butyl rubber stoppers for shore-based chemical and isotopic analysis of total dissolved carbonate ($\Sigma CO_2 = H_2CO_3^* + HCO_3^- + CO_3^{2-}$), CH_4, and other short-chain hydrocarbons including ethane and propane. The butyl rubber stoppers were pre-treated by boiling in 1 M NaOH to remove hydrocarbon contaminants present in the rubber. The concentrations of CO_2 were determined onshore after acidification of fluids with 25 wt.% phosphoric acid by injecting aliquots of headspace gas directly onto a gas chromatograph with a Porapak-Q packed column and a thermal conductivity detector. These data were corrected to account for CO_2 partitioning between the headspace and fluid phases within an individual serum vial. Concentrations of low molecular weight hydrocarbons were determined by purge-and-trap gas chromatography using a Porapak-Q packed column and a flame ionization detector. Fluid aliquots were flame-sealed in glass ampoules for stable hydrogen (δD_{H2O}) and oxygen ($\delta^{18}O_{H2O}$) isotope analysis. Concentrations are expressed in units of mmol/L fluid for aqueous species analyzed at sea or mmol/kg fluid for species analyzed in shore-based laboratories. Estimates of overall analytical uncertainties (2s) are ±10% for H_2, CH_4, C_2H_6, ΣH_2S, Sr, Li, Rb, Cs, Ba, Fe, and Al concentrations, ±5% for ΣCO_2, Mn, Br, and F concentrations, ±3% for Na, Mg, Cl, Ca, K, and SO_4 concentrations, ±2% for SiO_2 concentrations, and ±0.02 units for $pH_{25°C}$.

The stable carbon and hydrogen isotope compositions of ΣCO_2 and CH_4 were analyzed by isotope ratio monitoring - gas chromatography mass spectrometry (irm-GCMS) using a Finnigan DeltaPlus mass spectrometer interfaced to an Agilent 6890 gas chromatograph through a Finnigan Gas Chromatograph Combustion Interface III combustion interface held at 950 °C with a constant oxygen trickle. The pooled standard deviation (2s) for both $\delta^{13}C_{CO2}$ and $\delta^{13}C_{CH4}$ values is 0.6‰. The ^{34}S content of aqueous ΣH_2S and ΣSO_4 were determined following precipitation as Ag_2S and $BaSO_4$, respectively, using an automated elemental analyzer interfaced with an isotope ratio mass spectrometer. Analytical uncertainty for $\delta^{34}S$ values was ±0.3‰ (2s). Oxygen isotope compositions of vent fluid H_2O were analyzed using an automated CO_2 equilibration device on a VG Optima mass spectrometer. Hydrogen isotope compositions of vent fluid H_2O were analyzed as H_2 on a Finnigan MAT 252 mass spectrometer using the Zn reduction technique (Kendall and Coplen, 1985) to prepare H_2 following salt removal by vacuum distillation. Analytical uncertainty (2s) for δD_{H2O} and $\delta^{18}O_{H2O}$ values were estimated to be 3‰ and 0.2‰, respectively. $^{87}Sr/^{86}Sr$ values were determined for a subset of samples on a Finnigan MAT 261 thermal ionization mass spectrometer using static multi-collection (additional details in Eickmann et al., 2009). Analytical uncertainty for $^{87}Sr/^{86}Sr$ values is estimated at 0.00007 (2s) based on three individually processed aliquots of IAPSO reference seawater. With the exception of $^{87}Sr/^{86}Sr$, all stable isotope data are reported using standard delta notation. For the isotope A of interest, δA is defined by the expression:

$$\delta A\ (‰) = \frac{R_S - R_{STD}}{R_{STD}} \times 1000$$

where R_S and R_{STD} are the isotope ratios of the sample and standard, respectively. $\delta^{13}C_{CO2}$ and $\delta^{34}S_{SO4}$ are expressed relative to the V-PDB and V-CDT scales, respectively, whereas $\delta^{18}O_{H2O}$ and δD_{H2O} values are both expressed relative to the V-SMOW scale.

4. RESULTS

The overall composition of the smoker-type fluids presented here is in many ways similar to seawater-derived vent fluids from other back-arc and mid-ocean ridge environments (Fouquet et al., 1993; German and Seyfried, 2014; Reeves et al., 2011; Takai et al., 2008; Von Damm, 1995). Such fluids are typically characterized by near-zero Mg concentrations due to extensive fluid-rock interaction in high temperature reaction zones (Seyfried, 1987; Von Damm et al., 1985a), and are consistent with the near-zero Mg concentrations observed in most of the smoker fluids from SuSu

Knolls. Accordingly, it is assumed that measured non-zero Mg concentrations in sampled fluids reflect mixing of a zero-Mg endmember hydrothermal fluid with seawater prior to, or during, sampling in near seafloor environments. Zero-Mg samples are never collected, however, owing to the dead volume of samplers that is prefilled with bottom seawater. In some cases, inadvertent entrainment of ambient bottom seawater during sampling also occurs. The compositions of Mg-free endmember fluids (Table 1) were calculated by assuming conservative mixing and extrapolating the measured concentrations of a given species (Table S1) to a zero-Mg value using a least squares linear regression forced through seawater composition. Strontium isotope endmember values were calculated similarly by extrapolating the measured molar $^{87}Sr/^{86}Sr$ and Mg/Sr ratios to zero-Mg using a least squares linear regression forced through seawater composition (Albarède et al., 1981).

Measured Mg concentrations for the smoker-type fluids are, in general, greater than the 1.6 mmol/kg concentration expected for the 4 ml dead-volume of the isobaric gas-tight samplers (Seewald et al., 2002) and 0.27 mmol/kg expected for the 3.8 ml dead volume of the 'major' samplers (Von Damm et al., 1985a). Although this could reflect entrainment of ambient seawater during collection of the samples, we believe this is unlikely based on past experience at other vent sites (*c.f.* Cruse et al., 2008; Cruse and Seewald, 2010; Mottl et al., 2011). Moreover, replicate samples from several vents give nearly identical Mg concentrations that are above the dead volume value (Table S1), an unlikely consequence of a random process such as seawater entrainment. A more likely explanation for reproducible Mg concentrations that are above the dead volume value is that the fluids contained non-zero Mg concentrations when they exited the seafloor due to subsurface mixing with seawater. A similar phenomenon has been observed in focused-flow fluids from the nearby PACMANUS vent field (Reeves et al., 2011).

4.1. Major Species and pH

Endmember Cl concentrations were enriched in all smoker-type fluids relative to seawater (540 mmol/kg) and showed a high degree of variability within a given vent field (Table 1). For example, endmember Cl concentration varied from 620–712 mmol/kg and 550–739 mmol/kg at Suzette and North Su, respectively. Vent fluids at South Su were characterized by endmember concentrations of 609 and 620 mmol/kg, values that are within the range observed at the other vent areas. Replicate fluid samples from the NS6 vent at North Su showed variable concentrations that varied from 682–739 mmol/kg. This fluid had a measured temperature of 325 °C which is very close to the two-phase boundary for seawater at at 329 °C for a seafloor pressure of 118 bar (Bischoff and Rosenbauer, 1985). The fluid also displayed a flame-like flashing phenomenon upon exiting the chimney orifice, consistent with phase-separation. Accordingly, variations in the measured Cl concentrations of the NS6 fluid likely reflect differences in the relative proportion of brine and vapor collected during each sampling event due to active phase separation at the seafloor.

Because Na is the predominant cation in seawater, charge balance constraints require that endmember Na concentrations are closely linked to variations in Cl. Accordingly, except for fluid NS5 with a Na concentration of 454 mmol/kg, all smoker-type fluids are enriched relative to seawater (462 mmol/kg) with concentrations varying from 492–598 mmol/kg. Na/Cl ratios (Table 1), however, reveal values that are consistently below the seawater ratio of 0.86, indicating that Cl is more enriched than Cl.

Endmember K concentrations vary from 48–65 mmol/kg and are substantially enriched relative to seawater abundance (9.9 mmol/kg). For a given vent field, the highest K concentrations are associated with the most Cl-rich fluids (Table 1). Except for fluid NS4, endmember Ca concentrations are also enriched relative to seawater, but are characterized by a broader range of values from 21–51 mmol/kg. Relative to the other vents, the endmember Ca concentration of 3.6 mmol/kg at NS4 is substantially depleted and atypical for ridge-crest hydrothermal fluids that, in general, are enriched in Ca relative to seawater (Von Damm, 1995; German and Seyfried, 2014).

In contrast to the major cations, aqueous concentrations of SiO_2 do not vary systematically with Cl. Endmember SiO_2 concentrations in most fluids from each vent field show a similar range, varying from 13.3–17.8 mmol/kg. The endmember NS4 fluid, however, contains 29.2 mmol/kg SiO_2, substantially higher than the other vent fluids at SuSu Knolls (Table 1, Fig. 3).

High-temperature endmember ridge-crest vent fluids typically contain near-zero concentrations of aqueous SO_4, similar to Mg (Von Damm et al., 1985a; Seyfried, 1987). The abundance of aqueous SO_4 in the SuSu Knolls fluids provides additional evidence for endmember fluids mixing with normal seawater in subseafloor cavities or fractures. If hydrothermal fluids contain zero Mg and SO_4, conservative mixing with ambient seawater should produce a linear correlation between Mg and SO_4 that defines a line from the origin to seawater composition. Examination of Fig. 4, however, indicates that except for NS4, measured SO_4 concentrations are generally at or below values expected for conservative mixing. Extrapolation of the Mg-SO_4 trendlines to zero Mg yields negative SO_4 concentrations that are not meaningful.

The observed SO_4 depletions are consistent with subsurface SO_4 removal by anhydrite ($CaSO_4$) precipitation due to its low retrograde solubility at elevated temperatures (Bischoff and Seyfried, 1978; Holland and Malinin, 1979). Because anhydrite precipitation removes one mole of Ca for each mole of SO_4, endmember Ca concentrations calculated by extrapolation to zero Mg (Table 1) may systematically underestimate actual endmember values. However, the maximum observed vent fluid Mg concentration of 7.9 mmol/kg at vent SZ4 corresponds to a SO_4 depletion of only 2.8 mmol/kg, suggesting the endmember Ca concentrations are affected to a relatively minor degree.

An endmember ΣSO_4 concentration of 16.4 mmol/kg at the NS4 vent suggests that ΣSO_4 did not behave conservatively at this site during subsurface seawater mixing or the endmember fluid did not contain a near-zero ΣSO_4 concentration. The elevated ΣSO_4 abundance in conjunction with

Table 1

Endmember concentrations[*] of aqueous species in vent fluids from SuSu Knolls vent fields.

Field	T_{max}	pH_{min}	Na	K	Li	Rb	Cs	Ca	Sr	$^{87}Sr/^{86}Sr$	Fe	Mn	Al	Cl	Br	F	SiO_2	H_2	ΣH_2S	$\delta^{34}S_{H2S}$	CH_4	$\delta^{13}C_{CH4}$	C_2H_6	ΣCO_2	$\delta^{13}C_{CO2}$	$\delta^{18}O_{H2O}$	δD_{H2O}
Vent	°C	25 °C	mm	mm	mm	µm	µm	mm	mm	molal	mm	mm	µm	mm	mm	µm	mM	µM	mM	‰$_{VCDT}$	µM	‰$_{VPDB}$	µm	mm	‰$_{VPDB}$	‰$_{VSMOW}$	‰$_{VSMOW}$
Suzette																											
SZ1	303	3.7	508	48.0	0.73	49	2.2	33.8	0.26	0.70429	0.75	0.272	4	623	0.98	64	14.9	12	1.8	−5.1	528	−29.8	nd	16.3	0.1	0.8	−6
SZ2	274	3.6	528	49.1	0.80	48	2.5	49.4	0.39	nd	0.78	0.366	5	684	1.1	80	14.0	7.4	1.8	nd	221	−28.6	1.3	21.5	−0.2	1.4	−5
SZ3	290	3.5	539	49.0	0.81	44	2.5	47.9	0.39	nd	0.88	0.335	5	689	1.1	82	13.9	13	1.9	−5.9	184	nd	nd	17.4	−0.3	0.8	−1
SZ4	229	3.6	527	54.9	0.77	55	2.6	44.1	0.36	nd	0.52	0.325	1	677	1.0	66	13.7	7.7	1.3	nd	459	−32.0	nd	24.0	−0.9	1.1	1
SZ5	249	2.2	521	48.6	0.72	48	2.2	26.0	0.24	0.70501	4.3	0.273	18	620	0.95	533	16.1	8.0	5.3	−5.8	564	−31.0	3.1	17.8	−0.3	0.7	−3
SZ6	226	3.7	550	51.6	0.81	51	2.6	51.2	0.42	nd	0.38	0.378	2	712	1.1	86	13.3	37	1.2	nd	107	−28.4	0.65	17.8	0.1	0.7	−2
North Su																											
NS3	300	3.4	546	65.0	0.86	66	2.9	31.2	0.24	nd	2.3	0.425	10	674	1.1	145	17.8	82	3.4	−6.7	313	nd	2.6	11.9	−0.9	1.0	−1
NS4	241	1.5	492	49.0	0.71	54	2.5	3.6	0.059	0.70520	4.7	0.359	278	580	0.84	919	29.2	64	11.1	−4.7	853	nd	nd	28.1	−0.9	1.2	−3
NS5	299	3.2	454	49.4	0.67	51	2.3	20.6	0.24	nd	4.1	0.474	10	550	0.82	188	17.4	85	6.6	−6.9	639	−34.2	4.8	22.1	−0.3	0.7	−2
$NS6_{high\ Cl}$	325	2.8	598	64.9	0.90	64	3.1	37.7	0.43	0.70440	5.8	0.468	8	739	1.1	343	16.5	21	4.3	−6.1	93	nd	nd	7.2	nd	0.9	−2
$NS6_{low\ Cl}$	325	2.8	558	59.2	0.85	61	2.9	34.9	0.40	nd	5.8	0.481	6	682	1.0	333	nd	nd	nd	nd	nd	nd	nd	nd	nd	nd	nd
South Su																											
SS1	271	2.6	509	48.4	0.63	48	2.3	29.5	0.40	0.70450	2.2	0.558	8	620	0.94	385	15.1	15	6.2	−4.6	24	−19.9	0.070	142	−1.5	0.8	−2
SS2	288	2.7	498	48.6	0.63	50	2.0	27.7	0.30	nd	2.6	0.490	8	609	0.92	286	15.1	13	8.1	−4.6	24	−19.2	0.003	153	−1.7	0.9	−1
Seawater	3	7.9	462	9.9	0.028	1.3[b]	0.0023[b]	10.5	0.091	0.70916	1×10^{-6}	5×10^{-6}	0.03	540	0.81	64	0.13[a]	0	0	nd	0	nd	0.000	2.3	0.3[c]	−0.17[d]	−0.14[e]

nd = not determined.

[a] WOCE data from www.eWOCE.org.

[b] Spencer et al. (1970).

[c] Craig (1969).

[d] Craig and Gordon (1965).

[e] Redfield and Friedman (1965).

[*] mM = mmol/L fluid, mm = mmol/kg fluid, µM = µmol/L fluid, µm = µmol/kg fluid, nm = nmol/kg fluid. Tmax = maximum measured vent temperature. pHmin = lowest measured (25 °C) pH.

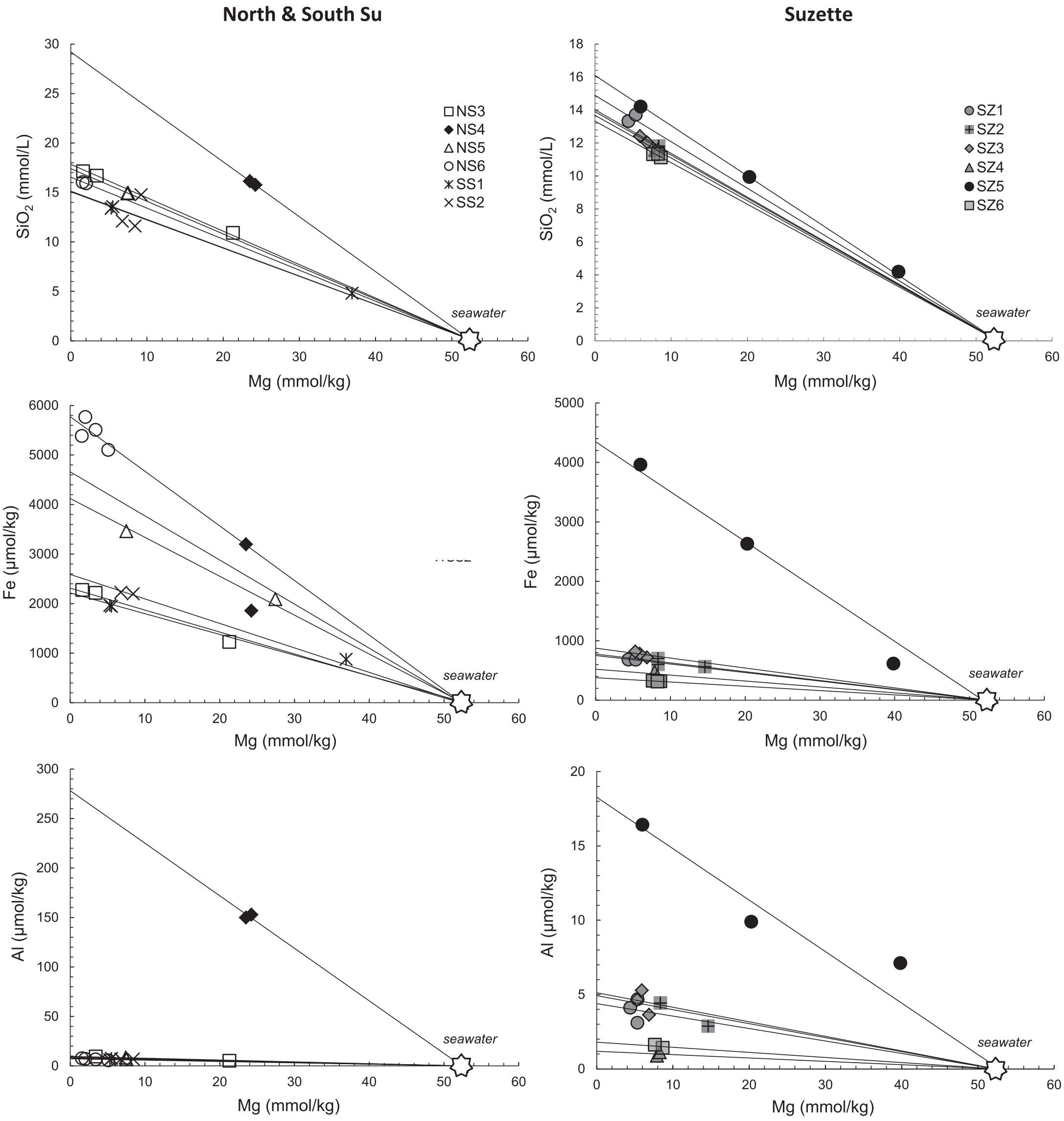

Fig. 3. Dissolved concentrations of SiO_2, Fe, and Al versus dissolved Mg in seawater-derived hot-spring fluids from areas of hydrothermal venting at SuSu Knolls. The open star indicates the composition of seawater which was included in the linear regressions indicated by the solid lines.

a relatively low endmember Ca abundance (3.6 mmol/kg) suggests that anhydrite dissolution is not the source of the additional ΣSO_4.

Except for a few samples, measured values of $\delta^{34}S_{SO4}$ for dissolved ΣSO_4 in the SuSu Knolls samples average 20.3‰, consistently lower than, but close to normal seawater SO_4 ($\delta^{34}S_{SO4} = 20.99 \pm 0.08$‰, Rees et al., 1978), suggesting a seawater origin (Table S1). Values of $\delta^{34}S_{SO4}$ that are slightly less than seawater are likely the result of anhydrite-$SO_{4(aq)}$ isotope fractionation during anhydrite precipitation (Thode and Monster, 1965; Van Driessche et al., 2016). Values of $\delta^{34}S_{SO4}$ significantly lower than 20‰ may indicate oxidation of H_2S which is depleted in ^{34}S relative to SO_4 (Table 1).

Measured $pH_{25°C}$ in the vent fluids cannot be extrapolated to zero Mg endmember values because pH is not a conservative property during fluid mixing. Accordingly, the lowest measured $pH_{25°C}$ values, which are associated with the lowest Mg fluids for a given vent, are reported in Table 1. Measured $pH_{25°C}$ at Suzette varied from 2.3–3.7, while $pH_{25°C}$ at North Su and South Su varied from 1.5–3.4 and 2.6–2.7, respectively. In general, the $pH_{25°C}$ values are higher than observed for the acid-sulfate fluids at North Su (Seewald et al., 2015).

4.2. Trace elements

The abundances of alkali trace elements Li, Rb, and Cs are substantially enriched in the endmember fluids relative to seawater, varying from 0.63–0.99 mmol/kg, 44–66 μmol/kg, and 2.0–3.1 μmol/kg, respectively. Except for Li, which is slightly lower in the fluids from South Su,

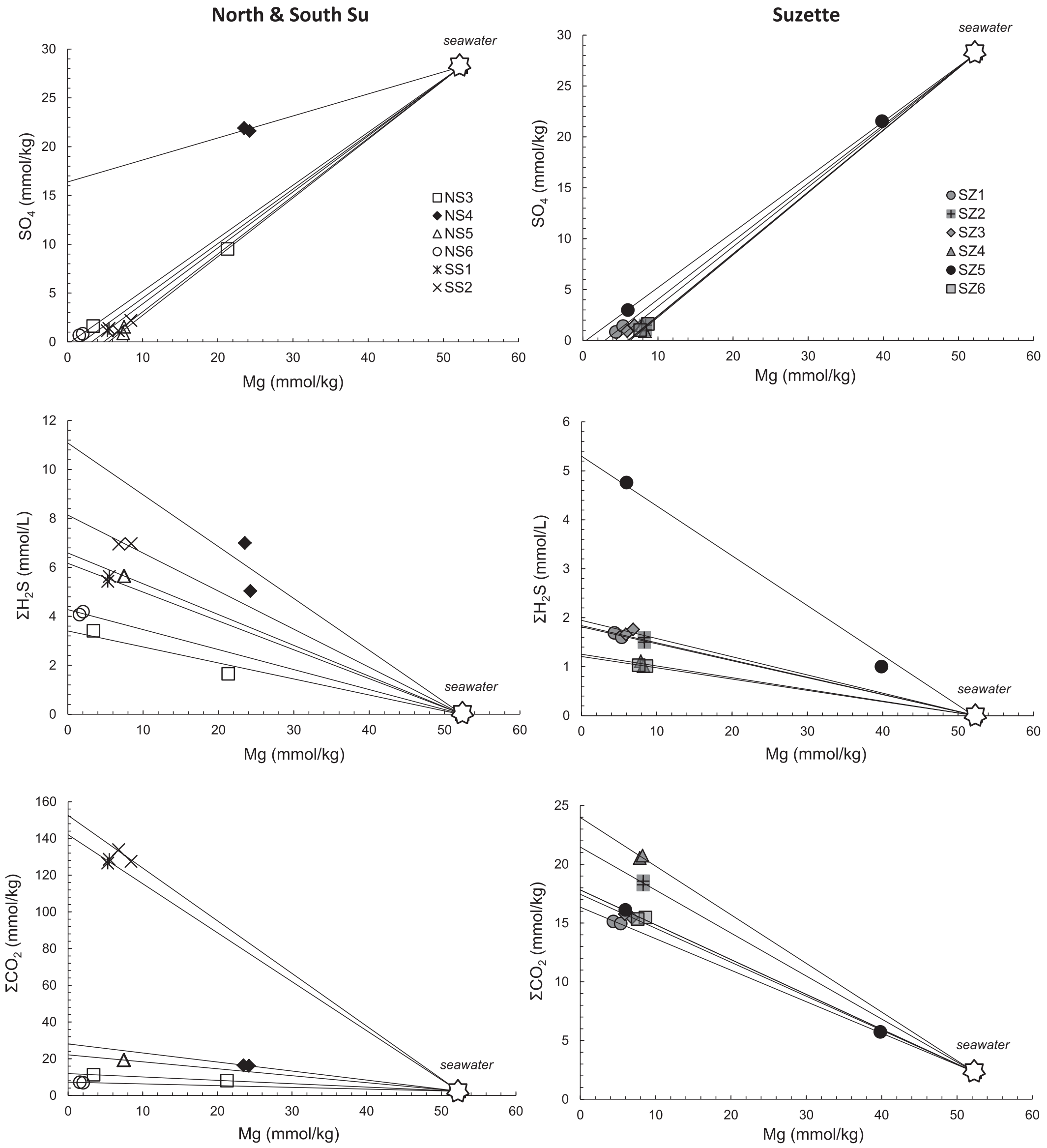

Fig. 4. Dissolved concentrations of SO_4, ΣH_2S, and ΣCO_2 versus dissolved Mg in seawater-derived hot-spring fluids from areas of hydrothermal venting at SuSu Knolls. The open star indicates the composition of seawater which was included in the linear regressions indicated by the solid lines.

systematic spatial variation between vent fields at SuSu Knolls is not apparent.

In general, the abundance of aqueous Sr tracks with aqueous Ca during hydrothermal alteration of the oceanic crust due to substitution in calcic phases such as anhydrite, plagioclase, and epidote (Berndt et al., 1988). Accordingly, it is not surprising that the Ca-poor fluid at NS4 is characterized by the lowest observed endmember Sr concentration of 0.059 mmol/kg, whereas the other relatively Ca-rich fluids at SuSu knolls show higher concentrations that vary from 0.24–0.43 mmol/kg. The assumption of conservative mixing of seawater and endmember vent fluids may not be appropriate for Sr due to anhydrite precipitation, and calculated endmember concentrations likely underestimate actual values due to Sr co-precipitation.

Endmember fluid $^{87}Sr/^{86}Sr$ values ranged from 0.70429–0.70520. These ratios are similar to the $^{87}Sr/^{86}Sr$ value of 0.7039 for crustal rocks at SuSu Knolls (Park et al., 2010), but substantially lower than the seawater value of 0.70916.

Endmember aqueous Br concentrations ranged from the near seawater abundance of 0.82 mmol/kg to values of 1.1 mmol/kg, and systematically varied with the concentration of Cl (Table 1). Endmember Br/Cl values were at or slightly above seawater values. Endmember F concentrations were also at or above seawater values of 64 μmol/kg, but showed substantial variability, reaching values as high as 919 μmol/kg in the NS4 fluid.

The smoker fluids at SuSu Knolls are highly enriched in Fe and Mn relative to seawater. Endmember Fe for example, ranged from 2.2–5.8 mmol/kg at North and South Su and, except for the SZ5 fluid that contained 4.3 mmol/kg, from 0.380.88 mmol/kg at Suzette (Table 1, Fig. 3). Endmember Mn abundances at SuSu Knolls show less variability, ranging from 0.316–0.558 mmol/kg at North and South Su and 0.272–0.378 mmol/kg at Suzette. Unlike Fe, aqueous Mn at SZ5 (0.273 mmol/kg) was not enriched relative to the other fluids. Aqueous Al concentrations show similar spatial trends as Fe, with most of the North and South Su fluids containing 6–10 μmol/kg Al, while the majority of Suzette fluids contained 1–5 μmol/kg Al. In contrast, the NS4 and SZ5 fluids were highly enriched in Al with concentrations of 278 and 18 μmol/kg, respectively (Table 1, Fig. 3).

4.3. Dissolved gases

Measurable concentrations of dissolved H_2 attest to the highly reducing nature of the smoker fluids at SuSu Knolls. Endmember concentrations at Suzette and South Su show a similar range of values from 7.4–37 μmol/kg while the North Su fluids contain slightly higher H_2 abundances, with endmember concentrations varying from 21–82 μmol/kg (Table 1).

Dissolved ΣH_2S abundances are similar at North and South Su, varying from 3.4–8.1 mmol/kg in most fluids. The majority of fluids at Suzette contain ΣH_2S abundances between 1.2 and 1.9 mmol/kg. The more acidic fluids from NS4 and SZ5 are enriched in dissolved ΣH_2S relative to the nearby fluids, with ΣH_2S concentrations of 11.1 and 5.3 mmol/kg, respectively (Table 1, Fig. 4). Values of $\delta^{34}S$ for aqueous ΣH_2S were between −6.9 and −4.6‰ (Table 1).

The abundance of volatile carbon species (ΣCO_2, CH_4, and C_2H_6) shows substantial inter-field differences (Table 1, Fig. 4). Endmember ΣCO_2 concentrations range from 142–153 mmol/kg at South Su, but only 7.2 to 28.1 mmol/kg at North Su and Suzette. The carbon isotopic composition of ΣCO_2 is characterized by a narrow range of endmember $\delta^{13}C$ values from −1.7 to 0.1‰. Dissolved CH_4 abundances show opposite inter-field trends relative to ΣCO_2, with the South Su fluids containing 24 μmol/kg CH_4, while the North Su and Suzette fluids contain 93–639 μmol/kg. The low CH_4 abundance at South Su is accompanied by a relatively enriched carbon isotope composition of −19.2‰, while the more abundant CH_4 at North Su and Suzette is more depleted with $\delta^{13}C$ values ranging from −34.2 to −28.4‰. The concentration of C_2H_6 varied from 0.003–4.8 μmol/kg, with the highest concentrations observed in the North Su fluids. Propane (C_3H_{10}) was detected in some of the samples, but at a level too low to quantify. Alkanes with chain lengths longer than propane were below detection.

4.4. Oxygen and hydrogen isotopes

Relative to seawater, the endmember smoker-type fluids are enriched in ^{18}O, with $\delta^{18}O$ values within the narrow range of 0.7–1.4‰ (Table 1). Endmember δD values of the fluids vary from −6 to 1‰, indicating that within the error of the analysis, the smoker-type fluids are the same or depleted in D relative to seawater.

5. DISCUSSION

Convective circulation of seawater-derived hydrothermal fluids at oceanic spreading centers results in extensive chemical exchange and mineralogical alteration of the lithosphere. Early-stage reactions during seawater recharge involve precipitation of Mg as aluminosilicate minerals and SO_4 as anhydrite ($CaSO_4$) as fluids penetrate to increasing depths and are progressively heated (Seyfried, 1987). Fluids venting at the seafloor may attain temperatures near 400 °C and are characterized by near-zero concentrations of Mg and SO_4 and substantial enrichments in the abundance of Ca, K, SiO_2, mobile trace elements, H_2, ΣH_2S, ΣCO_2, sulfide forming metals, and acidity relative to seawater (German and Seyfried, 2014). Fluids from back-arc environments are characterized by a broad range of compositions that show significant overlap with fluids from basalt-hosted mid-ocean ridge environments, but in many cases are more acidic and metal-rich (Fouquet et al., 1993; Gamo et al., 1997; Douville et al., 1999a,b; Takai et al., 2008; Mottl et al., 2011; Reeves et al., 2011). It has been postulated that the low pH and high transition metal abundances reflect a contribution of acidic magmatic volatiles to convecting seawater-derived fluids (Gamo et al., 1997; Takai et al., 2008; Mottl et al., 2011; Reeves et al., 2011).

The composition of SuSu Knolls smoker fluids suggests that convective circulation of seawater-derived fluids and water-rock reaction with the igneous crust can account for their formation (Fig. 1). For example, endmember smoker fluids contain near-zero concentrations of Mg and SO_4, are highly reducing, acidic, and metal- and sulfide-rich. Ratios of Na/Cl equal to or less than seawater values and substantial enrichment of Ca in the SuSu Knolls fluids are similar to observations from basalt-hosted systems.

In contrast to Na, the abundance of other alkalis (K, Rb, Cs, and Li) show large enrichments in the SuSu Knolls Smoker fluids relative to seawater. Because K, Rb, Cs, and Li readily partition into the aqueous phase during fluid-rock interaction at high temperatures, their aqueous concentrations in ridge-crest hydrothermal fluids typically reflects their abundance in unaltered oceanic lithosphere (Seyfried et al., 1984; Von Damm, 1995; Mottl et al., 2011; Reeves et al., 2011). Accordingly, concentrations of K, Rb, Cs, and Li in the SuSu Knolls fluids that are higher than abundances typically observed in basalt-hosted mid-ocean ridge vent fluids is consistent with the presence of alkali-rich felsic crust at SuSu Knolls. Assuming Rb, Cs, and Li are not incorporated into secondary alteration phases and quantitatively partition into the aqueous phase during fluid-rock interaction, water/rock mass ratios can be calculated from the concentrations of these elements in vent fluids and unaltered lithosphere. Using mid-range values for the Li, Rb, and Cs concentrations in volcanic rocks near SuSu Knolls (5–6 ppm Li, 3–24 ppm Rb, 0.2–1.0 ppm Cs;

Sinton et al., 2003; Beier et al., 2015) water/rock mass ratios of 0.9–3.6 are indicated for SuSu Knolls smoker fluids (Fig. 5). It should be recognized that these ratios only record the amount of fresh rock encountered by high temperature fluids and represent maximum values due to the assumption of 100% extraction efficiency. The low water/rock mass ratios indicate that fluid-rock interactions in subsurface reaction zones at SuSu Knolls are occurring under rock-dominated conditions, as is the case in other back-arc and mid-ocean ridge hydrothermal environments. Rock-dominated conditions facilitate buffering the activity of solubility controlled aqueous species by aluminosilicate mineral assemblages during fluid-rock interaction in deep-seated reaction zones (Bowers and Taylor, 1985; Berndt et al., 1989; Seyfried et al., 1991).

In addition to fluid-rock interaction, the composition of ridge-crest hydrothermal fluids may be strongly influenced by processes such as phase separation, subsurface mixing with seawater, and entrainment of magmatic volatiles released by an active magma chamber. All of these processes appear to occur in both mid-ocean ridge and back-arc environments. The degree to which these processes influence fluid chemistry is highly variable owing to differences in numerous variables such as temperature, pressure, rock composition and texture, and subsurface hydrology. All of these processes influence *in situ* pH, a key variable in the aqueous transport and deposition of sulfide minerals, and therefore play a critical role in the formation of metal sulfide deposits at and below the seafloor.

5.1. Chloride variability

Phase separation has been identified as an important process that influences the chlorinity of ridge-crest hydrothermal fluids (Butterfield et al., 1994, 2003; Von Damm et al., 1997; Seewald et al., 2003). Aqueous Cl concentrations that are enriched or depleted relative to seawater are typically attributed to formation and segregation of brine and vapor phases during phase separation under sub- or supercritical conditions. All endmember Cl concentrations in the SuSu Knolls smoker fluids are equal to or enriched relative to concentrations in seawater (Table 1). Measured temperatures of 325 °C at the NS6 vent place these fluids near the two-phase boundary of seawater at a seafloor depth of 1183 m (Fig. 6; Bischoff and Rosenbauer, 1985), consistent with collection of replicate fluid samples that contain variable Cl concentrations indicative of ongoing phase separation during upflow (Table S1). Other fluids at SuSu Knolls have measured temperatures that are substantially below those required for phase separation at seafloor pressures (Fig. 6). The non-zero Mg concentrations for some of these fluids when they exit the seafloor indicate that subseafloor mixing with cool ambient seawater has lowered temperatures from conditions that may have resulted in phase separation prior to mixing. If it is assumed that heat capacity remains constant with temperature (a simplifying assumption that affects estimated temperatures by <10 °C) and the measured temperatures are extrapolated to 1.6 mmol/kg Mg (seawater Mg occupying the sampler dead volume does not affect measured temperatures), endmember temperatures for some of the North and South Su vents are close to values

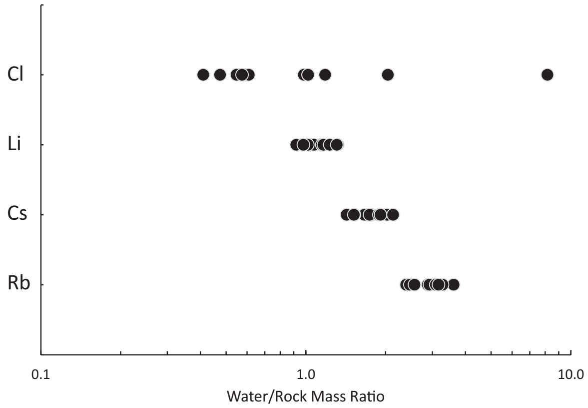

Fig. 5. Estimated water/rock mass ratios for seawater-derived hydrothermal fluids from areas of venting at SuSu Knolls based on the aqueous concentrations of dissolved Cl, Li, Cs, and Rb.

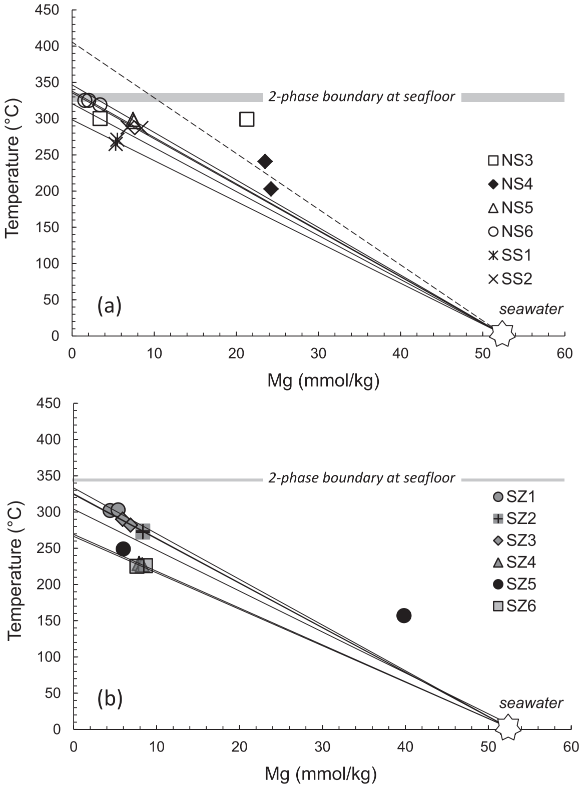

Fig. 6. Measured temperatures versus dissolved Mg in seawater-derived hot-spring fluids from areas of hydrothermal venting at SuSu Knolls in 2006. The open star indicates the temperature and composition of seawater. The width of shaded gray lines indicate the range of temperatures for the two-phase boundary of seawater at the seafloor depths for areas of venting at SuSu Knolls based on the equation of state for seawater derived by Bischoff and Rosenbauer (1985).

required for phase separation at near-seafloor conditions (Fig. 6).

Although there is clear evidence for phase separation at SuSu Knolls, it may not be the only mechanism modifying the chlorinity of smoker fluids. Entrainment of volatiles degassed from silicic magmas could potentially enrich or deplete seawater-derived vent fluids depending on the Cl-content of the magmatic fluid. However, based on the relatively low Cl content of magmatic fluids likely responsible for the formation of the acid-sulfate fluids at North Su (Seewald et al., 2015), this does not appear to be a viable mechanism for producing the Cl-enriched smoker fluids at SuSu Knolls. Leaching of Cl from crustal rocks is typically not invoked as a fluid enrichment mechanism in mid-ocean ridge vent systems due to the very low concentrations of Cl in mid-ocean ridge basalts, but has been invoked for hydrothermal systems at Lau Basin due to higher Cl concentrations in back-arc basalts and more felsic rocks (Mottl et al., 2011). Rocks collected at the seafloor in the vicinity of SuSu Knolls contain 0.18–0.40 wt.% Cl (Sinton et al., 2003; Beier et al., 2015). If it is assumed that Cl is highly mobile during hydrothermal alteration and partitions quantitatively into the aqueous phase, water/rock mass ratios of 0.5–8.2 are indicated for the Cl enrichments in SuSu Knolls vent fluids relative to seawater (Fig. 5). This range of values is generally consistent with water/rock mass ratios calculated based on alkali element concentrations and demonstrates that rock leaching is a viable mechanism to produce the observed Cl enrichments. It does not, however, preclude the possibility that phase separation has also influenced the chlorinity of the SuSu Knolls vent fluids.

Measured Cl concentrations in the actively phase separating NS6 fluids were above seawater values and showed substantial variability that reflects variable extents of phase segregation during sample collection. Observations of the temporal evolution of phase separated mid-ocean ridge hot-springs involve the initial venting of low-chlorinity vapors during active periods of phase separation followed by venting of Cl-rich residual brines stored in the crust as the system cools (Butterfield et al., 1997; Von Damm et al., 1997). Venting of actively phase separating high-Cl fluids at NS6 is anomalous in the context of such a model, unless they were enriched in Cl relative to seawater prior to phase separation. Leaching of rock-derived Cl from felsic crust, as described above, can produce this Cl-enriched fluid. Such an interpretation would suggest that Cl-rich fluids venting at NS6 represent a vapor-phase produced by phase separation of a fluid containing even higher Cl concentration. This implies that measured Cl concentrations may not be a reliable indicator of phase separation in back-arc environments where the crust contains significant Cl concentrations, and should be used with caution to assess the temporal evolution of hydrothermal activity.

5.2. Sediment interaction

Endmember dissolved CH_4 concentrations in the SuSu knolls smoker fluids show a high degree of variability, ranging from 24–853 μmol/L (Table 1). A variety of processes may contribute CH_4 to submarine hot-spring fluids including abiotic sources, microbial activity, and thermogenic production during sediment interaction (Welhan, 1988; Von Damm et al., 1985b, 2005; Seewald et al., 1990, 1994; Cruse and Seewald, 2006; Proskurowski et al., 2008; McDermott et al., 2015). Magmatic volatiles venting in acid-sulfate fluids at North Su contain very low levels of CH_4 (Seewald et al., 2015) suggesting that CH_4 in nearby smoker fluids is not derived from active degassing of a sub-seafloor magma chamber.

High CH_4 concentrations in several SuSu Knolls fluids, along with its isotopic composition, suggest derivation from thermal alteration of organic-bearing sediments. Variations in dissolved CH_4 concentrations are accompanied by systematic variations in stable carbon isotope ratios, with CH_4 in the high concentration fluids being characterized by more depleted $\delta^{13}C$ values relative to low concentration fluids (Fig. 7a). Hemipelagic sediments are abundant within a few hundred meters of the active hot-springs at SuSu Knolls (Hrischeva et al., 2007). The abundance and isotopic composition of CH_4 in the SuSu Knolls fluids can be accounted for by a model involving variable mixing of

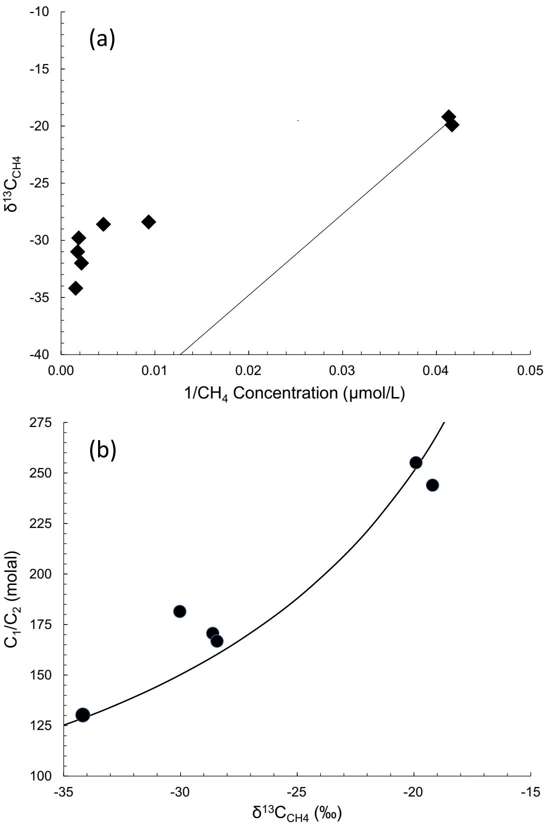

Fig. 7. Plot of the carbon isotopic composition of methane ($\delta^{13}C_{CH4}$) versus 1/CH_4 concentration (a) and the C_1/C_2 molal ratio versus $\delta^{13}C_{CH4}$ (b) for methane and ethane in hydrothermal fluids at SuSu Knolls. The solid line in (a) represents a linear regression of the data and in (b) defines the trend for mixing of thermogenic hydrocarbons characterized by a $\delta^{13}C_{CH4}$ value of −36‰ and a C_1/C_2 of 121 with abiotic hydrocarbons characterized by a $\delta^{13}C_{CH4}$ value of −7‰ and a C_1/C_2 of 2000.

isotopically depleted CH_4 produced thermogenically during hydrothermal sediment alteration with a relatively small amount of isotopically enriched CH_4 produced abiotically from mantle derived CO_2 during hydrothermal circulation or by leaching from rock-hosted fluid inclusions (Kelley, 1996; Kelley and Früh-Green, 1999; McDermott et al., 2015; Wang et al., 2018). A plot of $\delta^{13}C_{CH4}$ values and $1/CH_4$ concentration produces a linear trend with the y-intercept yielding a $\delta^{13}C_{CH4}$ value of −32‰ that defines the isotopic composition of the sedimentary endmember (Fig. 7a). Although the sedimentary endmember is more ^{13}C enriched than CH_4 observed in other sediment-influenced spreading centers, where $\delta^{13}C_{CH4}$ values vary from −40 to 55‰ (Welhan and Lupton, 1987; Lilley et al., 1993; Cruse and Seewald, 2006, 2010), it is similar to values typically observed for thermogenic CH_4 in conventional petroleum producing sedimentary basins (Schoell, 1988; Whiticar, 1999). The enriched $\delta^{13}C_{CH4}$ values for sediment-derived CH_4 in the SuSu Knolls fluids may reflect the absence of microbial methanogenesis that has been invoked as a source for a portion of the sedimentary CH_4 entrained by vent fluids in other ridge-crest systems (Whiticar et al., 1994; Cruse and Seewald, 2006; Kawagucci et al., 2011).

Measured concentrations of aqueous ethane (C_2H_6) also suggest hydrocarbon generation and entrainment in response to thermal alteration of sedimentary organic matter. The molal ratios of CH_4 to C_2H_6 (C_1/C_2) vary from 121 to 255 (Fig. 7b) and are consistent with relative hydrocarbon abundances from sediment covered spreading centers such as Guaymus Basin and Middle Valley (Welhan and Lupton, 1987; Cruse and Seewald, 2006). Moreover, C_1/C_2 molal ratios decrease systematically with decreasing values $\delta^{13}C_{CH4}$ (Fig. 7b), a trend consistent with mixing of a C_{2+}-rich thermogenic gas with a CH_4-rich abiotic gas produced from magmatic CO_2. High temperature vent fluids from the nearby sediment-free PACMANUS hydrothermal contain abiotic CH_4 of likely abiotic origin ($\delta^{13}C_{CH4}$ values of −7 to −15‰; Reeves et al., 2011), while the relative abundance of low molecular weight hydrocarbons in vent fluids from unsedimented spreading centers are characterized by C_1/C_2 molal ratios >2000 (McCollom and Seewald, 2007). Mixing thermogenic hydrocarbons characterized by a $\delta^{13}C_{CH4}$ value of −36‰ and a C_1/C_2 of 121 (the lowest values observed at SuSu Knolls) with putative abiotic hydrocarbons characterized by a $\delta^{13}C_{CH4}$ value of −7‰ and a C_1/C_2 of 2000 reproduces the systematic variation of C_1/C_2 with $\delta^{13}C_{CH4}$ observed in Fig. 7b.

Additional evidence for interaction of the SuSu Knolls smoker vent fluids with sediments is provided by the isotopic composition of dissolved ΣCO_2. Except for the fluids at South Su that are characterized by an average $\delta^{13}C_{CO2}$ value of −1.6‰, the carbon isotope composition of dissolved ΣCO_2 in the North Su and Suzette fluids display a narrow range of $\delta^{13}C_{CO2}$ values that vary from −0.9 to 0.1‰. The carbon isotopic composition of ΣCO_2 at North Su and Suzette is indistinguishable from the expected isotopic composition of marine carbonate that is abundantly present in hemipelagic sediments at SuSu Knolls (Hrischeva et al., 2007). Accordingly, dissolved ΣCO_2 in smoker fluids at North Su and Suzette may be derived entirely from dissolution of sedimentary carbonate.

Based on the calcite contents of 11–50 wt.% reported by Hrischeva et al. (2007) and the endmember ΣCO_2 concentrations (Table 1), fluid/sediment mass ratios of 90 to 950 would be required to account for range of ΣCO_2 concentrations observed in the North Su and Suzette smoker fluids. The isotopic composition of magmatically-derived ΣCO_2 actively degassing in nearby acid-sulfate fluids at North Su has an ^{13}C content of −2.9‰ (Seewald et al., 2015), significantly more depleted than the isotopic composition of CO_2 in the North Su and Suzette fluids. Thus, the low concentration of dissolved CO_2 in conjunction with its isotopic composition suggests that magmatic degassing has not contributed large quantities of CO_2-rich volatiles to the chemistry of smoker fluids venting at North Su and Suzette.

A different model emerges for South Su vent fluids. They are characterized by a more depleted $\delta^{13}C_{CO2}$ value of −1.6‰ and substantially higher endmember ΣCO_2 concentrations that vary from 142 to 153 mmol/kg fluid, suggesting addition of greater amounts of magmatic volatiles to the South Su fluids. Moreover, the low concentrations of CH_4 with a ^{13}C-enriched isotopic signature (−20‰) suggest that the extent of fluid-sediment interaction was substantially less at South Su than at North Su and Suzette, and represents a relatively minor source of ΣCO_2. Although a $\delta^{13}C_{CO2}$ value of −1.6‰ indicates ΣCO_2 that is slightly enriched in ^{13}C relative to magmatic ΣCO_2 in acid-sulfate fluids at North Su (−2.9‰; Seewald et al., 2015), it is consistent with magmatic ΣCO_2 in vent fluids from other back-arc environments where slab-derived CO_2 results in ^{13}C-enriched CO_2 in the overlying mantle (Takai et al., 2008; Mottl et al., 2011; Reeves et al., 2011). Local variations in the isotopic composition of magmatic CO_2 between the individual vent fields at SuSu Knolls is not unexpected due to isotopic fractionation during magma degassing in the shallow crust (Javoy et al., 1978; Mattey, 1991; Pester et al., 2012). Collectively, the abundance and isotopic composition of dissolved CO_2 in the SuSu Knolls vent fluids point to locally variable contributions of magmatic volatiles to the chemistry of smoker-type fluids.

5.3. Sources of acidity

Despite numerous compositional similarities between vent fluids at mid-ocean and back-arc spreading centers, there are important differences that reflect geochemical processes unique to back-arc environments. In particular, several SuSu Knolls fluids are characterized by $pH_{25°C}$ values in the range of ~2–3, significantly lower than the range of ~3–4 typically observed for mid-ocean ridge vent fluids (Fig. 8). Similar $pH_{25°C}$ values have been observed in high temperature vent fluids from other back-arc environments such as Pual Ridge (PACMANUS vent field) and Lau Basin, and arc environments such as Brothers Volcano on the Kermadec Arc (Fouquet et al., 1993; Takai et al., 2008; de Ronde, 2011; Mottl et al., 2011; Reeves et al., 2011). Many of these highly acidic back-arc fluids are more enriched in sulfide forming metals such as Fe, Zn, Cu, and Pb than those venting at mid-ocean ridges (Fouquet et al.,

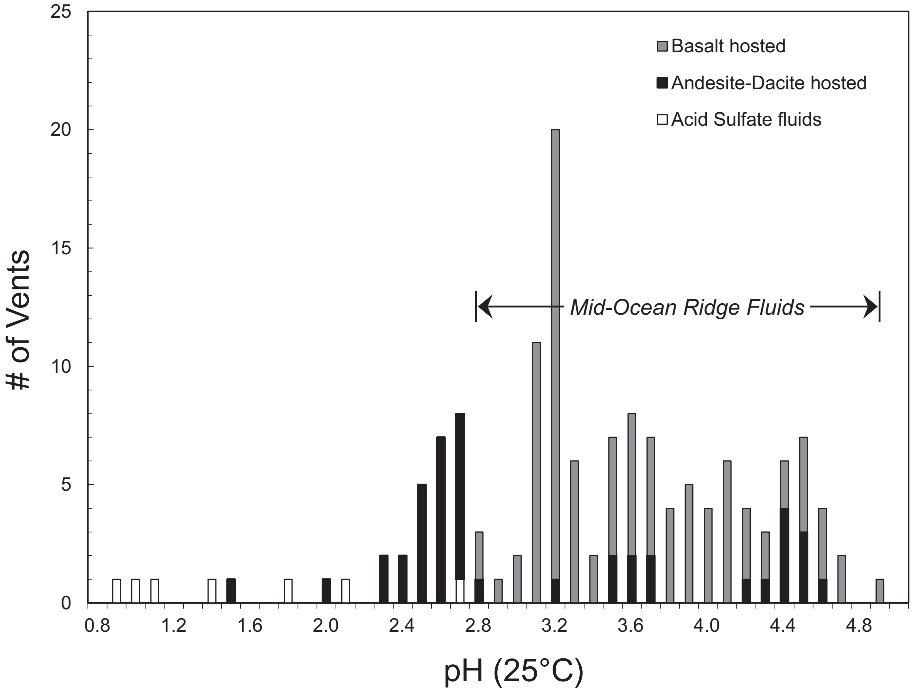

Fig. 8. Histogram showing the frequency of measured $pH_{25°C}$ values for submarine hydrothermal fluids at back-arc and mid-ocean spreading centers. Data are from Campbell et al. (1988); Fouquet et al. (1993); Butterfield and Massoth (1994); Gamo et al.(1997); Von Damm et al. (1985a, 1998, 2003, 2006); Von Damm and Bischoff (1987); Von Damm (2004); Takai et al. (2008); Mottl et al. (2011); Reeves et al., 2011; Pester et al. (2012); Seewald et al. (2015), this study.

1993; Craddock, 2008; Takai et al., 2008; Mottl et al., 2011; Reeves et al., 2011).

5.3.1. *Magmatic volatiles*

The high acidity and dissolved metal content of back-arc basin vent fluids has been used as evidence to support a contribution of SO_2-bearing magmatic volatiles to the chemistry of smoker fluids in arc and back-arc environments (de Ronde et al., 2005; Takai et al., 2008; Resing et al., 2007, 2009; Mottl et al., 2011; Reeves et al., 2011). Magmatic SO_2 represents a substantial source of acidity because it partitions into aqueous fluids exsolved from SO_2-bearing magmas (Scaillet and Pichavant, 2003) and disproportionates upon cooling to temperatures below 400 °C to produce reduced and oxidized sulfur species according to the reactions:

$$4SO_{2(aq)} + 4H_2O = H_2S_{(aq)} + 3H_2SO_{4(aq)} \quad (1)$$

$$3SO_{2(aq)} + 2H_2O = S^{\circ}{}_{(s)} + 2H_2SO_{4(aq)} \quad (2)$$

The relative importance of reactions (1) and (2) is strongly dependent on temperature, redox state, pH, and total sulfur (i.e. initial SO_2) present (Iwasaki and Ozawa, 1960; Holland, 1965; Drummond, 1981; Kusakabe et al., 2000; Seewald et al., 2015). Regardless of which reaction dominates, both produce acidity as H_2SO_4, which dissociates to HSO_4^- and H^+. SO_2-bearing magmatic fluids also contain substantial quantities of HCl and HF, in addition to CO_2 and H_2O, which may also influence the acidity of back-arc vent fluids. Elevated concentrations of CO_2 and F support a significant contribution of magmatic volatiles to some of the smoker-type fluids at SuSu Knolls and fluids from other back-arc environments (Fouquet et al., 1993; Takai et al., 2008; Mottl et al., 2011; Reeves et al., 2011).

Evidence for the addition of a magmatic fluid to the SuSu Knolls vent fluids is provided by the hydrogen and oxygen isotopic composition of H_2O (Table 1). Mid-ocean ridge hydrothermal fluids contain H_2O that is typically characterized by small enrichments in the heavy isotopes of hydrogen and oxygen relative to seawater (Shanks et al., 1995; Shanks, 2001). In contrast, the SuSu Knolls smoker fluids show similar minor enrichments in ^{18}O, but most samples are significantly depleted in D relative to seawater (Table 1). The range of oxygen and hydrogen isotopic compositions for H_2O in the SuSu Knolls smoker fluids is almost identical to that observed for smoker fluids at the nearby PACMANUS hydrothermal system (Reeves et al., 2011), suggesting similar contributions of magmatic H_2O. The isotopic composition of magmatic H_2O added to acid-sulfate fluids at SuSu Knolls (Seewald et al., 2015) has δD values from −26 to −31‰ and $\delta^{18}O$ from 6.5 to 8.3‰, consistent with the composition of H_2O estimated for subduction-related volcanic vapors (Giggenbach,1992; Hedenquist and Lowenstern, 1994). Isotopic mass balance constraints suggest that the SuSu Knolls and PACMANUS fluids may contain as much as 25 wt.% magmatic H_2O (Reeves et al., 2011), although substantially smaller contributions are possible due to the relatively large uncertainties associated with the hydrogen isotopic data used for the isotopic mass balance.

The potential impact of magmatic volatiles on the acidity of smoker type-fluids is readily apparent at the NS4 vent where fluids are characterized by a $pH_{25°C}$ value of 1.5, substantially lower than the other smoker fluids at North Su (Table 1). The low pH of the NS4 fluids is accompanied by ΣSO_4 concentrations that are highly elevated relative to values expected for conservative mixing of a SO_4-free hydrothermal endmember and seawater (Fig. 4). The NS4 fluids contain similar concentrations of Na, K, mobile trace elements Li, Rb, and Cs, and Cl, and higher concentrations of ΣCO_2 and F relative to the other smoker fluids at North Su, suggesting that the elevated ΣSO_4 abundance reflects late stage addition of magmatic volatiles to a seawater-derived smoker-type fluid in the shallow subsurface. The net result is the formation of a hybrid fluid that has compositional features of nearby acid-sulfate fluids and convective seawater-derived smoker fluids. Due to absence of fresh Ca-bearing dacite in highly altered upflow zones, ΣSO_4 persists in solution due to the limited supply of aqueous Ca necessary for anhydrite precipitation in the SO_4-free hydrothermal endmember prior to mixing. Highly depleted Ca concentrations in the NS4 fluids relative to the other fluids and seawater (Table 1) indicate significant subsurface anhydrite precipitation induced by the addition of magmatic ΣSO_4.

Although disproportionation of magmatic SO_2 during mixing of a magmatic fluid with a seawater-derived hydrothermal fluid may produce substantial quantities of ΣSO_4, elevated concentrations will not be realized in high temperature fluids if an adequate source of Ca is available to remove SO_4 from solution by precipitation as anhydrite. Requisite Ca is readily available if the magmatic fluid is added to the convecting fluid prior to, or during, reaction with fresh crustal rocks under rock-dominated conditions. Except for NS4, the absence of elevated ΣSO_4 concentrations in Ca- and CO_2-rich endmember smoker-type fluids at SuSu Knolls suggests that entrainment occurs relatively early, prior to or during reaction with relatively unaltered rock at low water/rock mass ratio (Fig. 1).

Extensive fluid-rock interaction following addition of magmatic volatiles has the potential to substantially influence all aspects of vent fluid chemistry, especially pH. Numerous observations suggest that the acidity of SuSu Knolls and other relatively low pH smoker-type fluids from back-arc environments is extensively modified by fluid-rock reactions following entrainment of acidic volatiles. In particular, vent fluid acidity would be expected to correlate with endmember ΣCO_2 concentrations because, in general, CO_2 is abundant in magmatic fluids from the Eastern Manus volcanic zone (Reeves et al., 2011; Seewald et al., 2015) and, being relatively unreactive in discharging hydrothermal fluids, represents a conservative tracer of magmatic volatile input. Indeed, at the nearby PACMANUS hydrothermal system Reeves et al. (2011) documented decreasing values of $\delta^{34}S$ for dissolved H_2S with increasing ΣCO_2 concentrations that reflect a greater extent of H_2S production by SO_2 disproportionation in CO_2-rich fluids. A plot of felsic-hosted back-arc vent fluids, however, reveals the absence of a correlation between measured $pH_{25°C}$ and endmember ΣCO_2 concentrations (Fig. 9), suggesting that the amount of entrained magmatic volatiles is not the primary control on pH in most fluids. The lack of correlation between magmatic volatile content and $pH_{25°C}$ is readily apparent in the Suzette fluids. The SZ5 fluid is characterized by a highly acidic $pH_{25°C}$ value of 2.3 relative to the other fluids that vary from 3.5 to 3.7, yet it contains an endmember ΣCO_2 concentration of 17.8 mmol/kg that is nearly identical to the ΣCO_2 abundances in the less acidic fluids (Fig. 4).

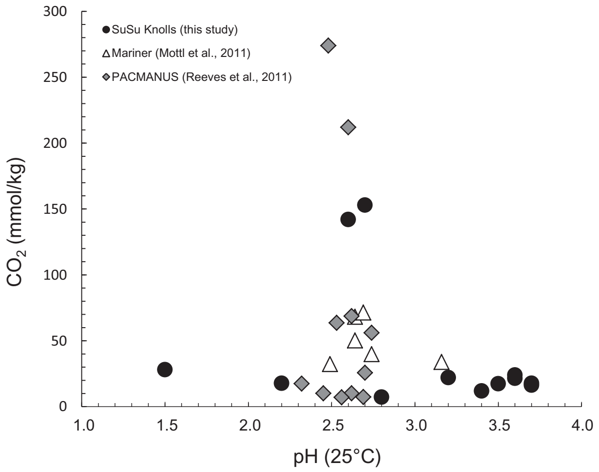

Fig. 9. Plot of endmember ΣCO_2 concentrations versus $pH_{25°C}$ for submarine hydrothermal fluids associated with degassing of silicic magma chambers at back-arc spreading centers. Data are from Mottl et al. (2011); Reeves et al. (2011); this study.

Compositional analysis of magmatic volatiles in acid-sulfate fluids at North Su and DESMOS indicate that the combined concentrations of magmatically derived H_2SO_4 and HCl exceed the abundance of CO_2 (Seewald et al., 2015). Accordingly endmember ΣCO_2 concentrations of 142 and 153 mmol/kg in the South Su smoker fluids would be accompanied by even greater concentrations of H^+ from the strong acids H_2SO_4 and HCl that would exceed the endmember ΣCO_2 concentrations and result in $pH_{25°C}$ values less than 1, far below the measured values of 2.6 and 2.7. The absence of acidity contributed by magmatic volatiles suggests that it has been titrated by fluid-rock reactions.

5.3.2. Fluid-mineral equilibria

The lack of correlation between magmatic volatile content and pH suggests that the pH of SuSu Knolls vent fluids is buffered by fluid-mineral equilibria in subsurface reaction zones following the addition of magmatic volatiles. Plagioclase-epidote-amphibole mineral assemblages have been shown to play an important role in regulating the pH of basalt-hosted mid-ocean ridge fluids (Seyfried, 1987, 1991; Berndt et al., 1989). The significantly lower pH observed in many back-arc vent fluids suggests that different mineral assemblage(s) regulate fluid acidity. The existence of oceanic crust in back-arc environments that is extensively altered to illite-pyrophyllite-anhydrite ± alunite assemblages formed during alteration by highly acidic fluids (Binns et al., 2007) represents a key difference in the mineralogy of subsurface upflow zones relative to mid-ocean ridge environments.

Phase relations in the system K_2O-Al_2O_3-SiO_2-H_2SO_4 can be used to assess the relationship between the composition of secondary mineral assemblages and fluid composition. Fig. 10 reveals that minerals such as pyrophyllite and K-alunite are stable at high H^+ activity while K-feldspar and muscovite (used here as a proxy for illite due to the absence of thermodynamic data) are stable at lower H^+ and high K^+ activities. Direct observation of altered substrate at SuSu Knolls is limited to surface samples that contain cristobalite, pyrite, native sulfur, kaolinite, and natroalunite/alunite (Binns et al., 1997; Yeats et al., 2014). Sediment gravity cores collected in the vicinity of the Suzette vent field also show the presence of alunite and clay minerals that are consistent with crustal alteration by highly acidic fluids (Hrischeva et al., 2007). Additional information on mineral assemblages likely to exist beneath the seafloor is available from the nearby PACMANUS hydrothermal system that was drilled during ODP leg 193 (Binns et al., 2007) and is characterized by fluid chemistry that is similar to SuSu Knolls (Reeves et al., 2011). Two distinct mineral assemblages are present, one composed of chlorite-feldspar-quartz, consistent with formation during interaction of fresh rock with a fluid of relatively high pH, and the other composed of quartz-illite-pyrophyllite-anhydrite ± alunite indicating formation from interaction with low-pH acid-sulfate-type fluids in upflow zones (Bach et al., 2003; Roberts et al., 2003; Binns et al., 2007).

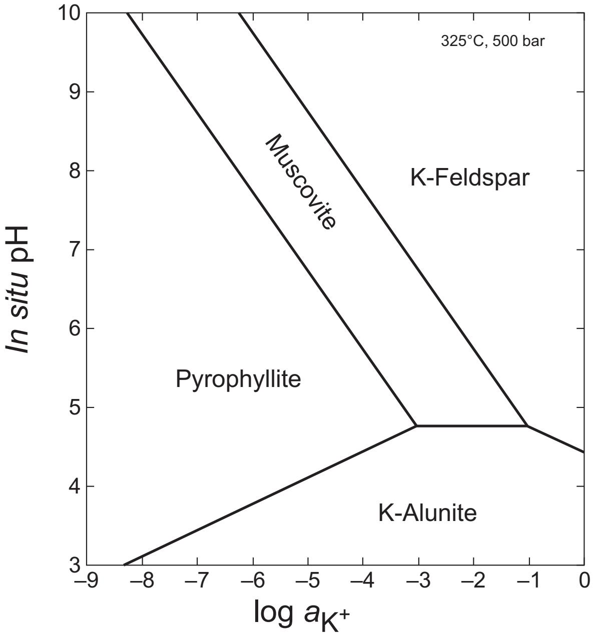

Fig. 10. Activity diagram showing phase relations in the system K_2O-Al_2O_3-SiO_2-H_2SO_4 at 325 °C, 500 bar, quartz saturation, and an aqueous SO_4^{2-} activity of 10^{-2}. Muscovite is used in the diagram as a proxy for illite due to the absence of reliable thermodynamic data for illite. Thermodynamic data necessary for the construction of this diagram are from Helgeson et al. (1978) and Shock and Helgeson (1988).

To assess the influence of magmatic volatiles and fluid-mineral chemical interaction on fluid pH, we used the EQ3NR/EQ6 (v. 8.0) reaction path computer code (Wolery, 1992; Wolery and Daveler, 1992) to simulate the reaction of a convective seawater-derived vent fluid containing entrained magmatic volatiles with fresh dacitic rock. The EQ3NR/EQ6 modeling software calculates the equilibrium composition and aqueous speciation of fluids and mineralogy during incremental reaction of fluid and rock with specified initial compositions. For this application, the minerals andalusite, kyanite, andradite, sillimanite, boehmite, corundum, and diaspore were suppressed for all calculations because they are not observed in the hydrothermal systems of the Eastern Manus Basin. The supporting thermodynamic database was generated at 25 MPa using SUPCRT92 software (Johnson et al., 1992) that included thermodynamic data for minerals (Helgeson et al., 1978) and relevant aqueous inorganic species (Shock and Helgeson, 1988; Shock et al., 1989, 1997; Sverjensky et al., 1997). Thermodynamic properties for Al^{3+} and aqueous aluminum complexes in the SUPCRT92 database were updated with values from Tagirov and Schott (2001). Illite is a common alteration mineral in back-arc hydrothermal environments, but was not included in the thermodynamic model due to the absence of reliable thermodynamic data necessary to assess its stability. Therefore, we allowed muscovite to form as an approximation of illite stability, recognizing that it is not present in back-arc hydrothermal environments and may be characterized by different thermodynamic properties.

The starting fluid composition used for our geochemical model reflects the mixing of a moderately acidic ($pH_{25°C} = 3.5$) seawater-derived hydrothermal fluid with the magmatic component of the NS2 acid-sulfate fluid venting at North Su as reported by Seewald et al. (2015) (Table 2). It was assumed that the weight fractions of seawater-derived hydrothermal fluid and magmatic fluid were 0.8 and 0.2, respectively. A total of 1 kg fluid was incrementally reacted with 1 kg of dacite (final water/rock mass ratio = 1) at 325 °C and 250 bar. These conditions were chosen to represent high temperature fluid-rock interaction in deep-seated reaction zones at SuSu Knolls where seawater-derived Mg and SO_4 would be have been previously removed by fluid rock reactions during recharge. Prior to fluid rock reaction, the mixed fluid is characterized by a $pH_{25°C}$ of 1 and a dissolved SO_4 concentration of 89 mmolal, reflecting the substantial contribution of acidity and ΣSO_4 from disproportionation of magmatic SO_2.

Fig. 11 illustrates the large changes in fluid chemistry that are predicted as a function of water/rock mass ratio. The *in situ* pH is highly acidic (~1.6) at water/rock mass ratios greater than 100 due to mass balance constraints that limit the capacity of the rock to buffer fluid chemistry. During this stage of reaction, quartz, Na-alunite, and anhydrite are the only minerals that form. As the fluid continues to react with increasing amounts of rock, decreasing water/rock mass ratios to values between 100 and 10, *in situ* pH increases sharply as acidity is titrated by mineral

Table 2
Comparison of fluid compositions predicted for re-equilbration of smoker fluids in hydrothermal upflow zones with natural vent fluid compositions at SuSu Knolls.

	Model #1	Model #2			Model #3		
	Start Fluid	Start Fluid (SZ1)	Pred. Equil.	SZ5	Start Fluid (NS3)	Pred. Equil.	$NS6_{high\ Cl}$
Temp. (°C)	325		272			325	
W/R (g/g)			1			1	
pH (25 °C)	1.0	3.7	2.0	2.2	3.4	2.8	2.8
pH (*in situ*)	1.6	4.1	2.4	2.4	4.2	3.5	3.5
K (mM)	48.0	48.0	45.7	48.6	65.0	55.2	64.9
Ca (mM)	40.0	33.8	23.7	26.0	31.2	30.7	37.7
H_2S (mM)	4.0	1.8	9.4	5.3	3.4	10.3	4.3
SiO_2 (mM)	12.0	14.9	14.7	16.1	17.8	12.3	16.5
Al (mM)	0.008	0.004	0.13	0.018	0.010	0.028	0.008
Fe (mM)	0.80	0.75	5.2	4.4	2.1	7.2	5.8
SO_4 (mM)	89.2	0	6.06	0	0	0.61	0
Solids	Dacite	Prl(40)-Qz(40)-Py(5)-$Alu^{†}$(15)	Prl-Crs-Py-Alu^{*}-Anh		Prl(45)-Qz(45)-Py(10)	Prl-Qz-Py-Ms-Anh	

Prl = pyrophyllite, Qz = quartz, Py = pyrite, Ms = muscovite, Anh = anhydrite, Alu = alunite solid solution, Crs = cristobalite.
(xx) = weight percent of mineral in assemblage.
mM = mmolal.
[†] Mole fraction Na-alunite = 0.70, Mole fraction K-alunite = 0.30.

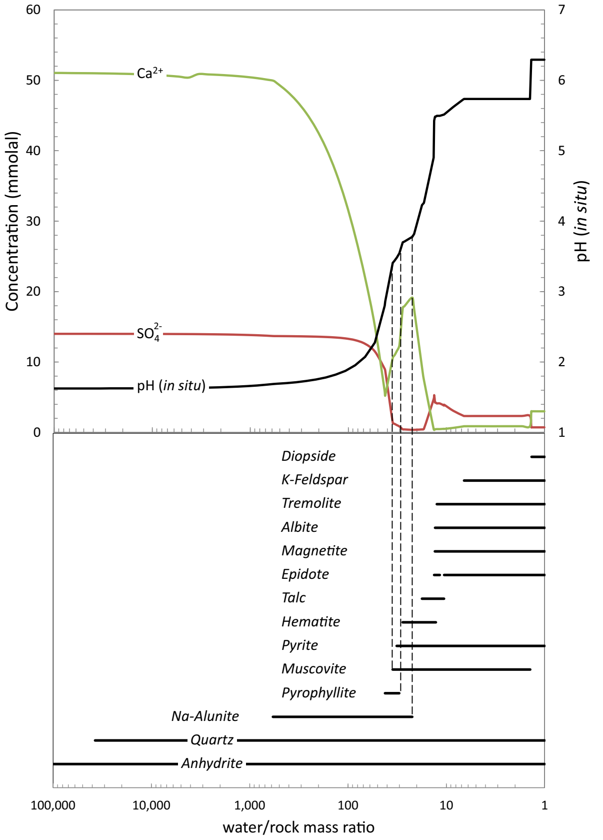

Fig. 11. Predicted concentrations of aqueous Ca and SO_4 and *in situ* pH (a) and the resulting secondary mineral assemblage (b) during reaction of a hydrothermal fluid containing acidic magmatic volatiles with dacite at 325 °C 250 bar as a function of water/rock mass ratio.

dissolution. Increasing *in situ* pH at lower water/rock mass ratios is accompanied by the sequential formation of aluminosilicate minerals in addition to pyrite and hematite (Fig. 11).

At water/rock mass ratios between 30 and 35, *in situ* pH experiences an inflection (Fig. 11), reflecting the formation of muscovite (illite) and the buffering of *in situ* pH at a value of ~3.5 by the assemblage pyrophyllite-muscovite (illite)-quartz according to the reaction:

$$\underset{\text{pyrophyllite}}{3Al_2Si_4O_{10}(OH)_{2(s)}} + 2K^+ = \underset{\text{muscovite (illite)}}{2KAl_3Si_3O_{10}(OH)_{2(s)}} + 2H^+ + \underset{\text{quartz}}{6SiO_{2(s)}} \qquad (3)$$

An *in situ* pH of 3.5 corresponds to a measured $pH_{25°C}$ of ~2.7, similar to measured values for many smoker vent fluids in back-arc environments. Although the model reproduces the low pH of smoker fluids in back-arc environments, it fails to explain measured concentrations of several aqueous species in SuSu Knolls and Suzette fluids. In particular, at water/rock mass ratios of 30–35, the model predicts aqueous Ca concentrations below 1 mmolal due to its removal from solution by anhydrite precipitation. Such low Ca concentrations are inconsistent with the abundance of aqueous Ca in endmember smoker fluids at SuSu Knolls where concentrations vary from 21–51 mmol/kg. The low predicted Ca concentrations at water/rock mass ratios of 30–35 occur in response to increased SO_4^{2-} activity as HSO_4^- dissociates to H^+ and SO_4^{2-} due to increased pH, which in turn greatly enhances the precipitation of anhydrite. Moreover, at water/rock ratios of 30–35, the reaction path model predicts elevated ΣSO_4 concentrations in excess of 6 mmolal, substantially greater than the natural fluids that contain near zero concentrations (Table 1, Fig. 4). Ca-rich, ΣSO_4-poor fluids are predicted by the model only at water/rock ratios less than ~13, when there is sufficient rock-derived Ca released to solution to remove magmatically-derived ΣSO_4 as anhydrite. However, at this water/rock ratio, the pyrophillite-muscovite (illite)-quartz mineral assemblage is no longer stable and *in situ* pH rapidly increases to a value between 5 and 6 (Fig. 11) which correspond to values of 3–4 at 25 °C. The reaction path model demonstrates the substantial capacity of unaltered dacitic rocks to buffer the pH of hydrothermal fluids at near neutral *in situ* values under rock-dominated conditions. Moreover, the results suggest that smoker-type fluids with a measured $pH_{25°C}$ below 3 are not the result of added magmatic volatiles during the reaction of seater-derived hydrothermal fluids with fresh dacite at low water/rock ratios.

An alternative model for the formation of lower pH smoker-type fluids in back-arc environments involves initial reaction of seawater-derived vent fluids with fresh crustal rocks under low water/rock mass ratios and subsequent reaction reaction with rocks previously altered by acid-sulfate fluids in hydrothermal upflow zones above an active or preexisting magma chamber. Quartz-illite-pyrophyllite-anhydrite ± alunite assemblages formed by acid-sulfate fluids will be in a state of disequilibrium during subsequent reaction with convective smoker-type fluid characterized by higher pH. Equilibrium at low water/rock ratio is attained by changes in fluid chemistry dictated by the mineralogy of the rocks owing to the substantially greater buffer capacity of minerals relative to aqueous fluids of near-seawater chlorinity on an equal mass basis. Therefore, equilibration of smoker-type fluid compositions with quartz-illite-pyrophyllite-anhydrite ± alunite assemblages formed at low pH will result in formation of low pH fluids until the buffering capacity of the mineral assemblage is exhausted.

The hydrothermal fluid compositions at SuSu Knolls provide compelling support for a model involving re-equilibration of smoker fluids with quartz-illite-pyrophyllite-anhydrite ± alunite assemblages during upflow. For example, all fluids sampled at Suzette are characterized by a very narrow range for the endmember abundances of Na, K, Rb, Cs, Li, Mn, ΣCO_2, and SiO_2 suggesting that they are derived from a common source fluid at depth that has entrained similar amounts of magmatic volatiles and interacted with fresh rock at low water/rock mass ratios (Table 1, Figs. 3 and 4). Endmember fluid from the SZ5 vent, however, is considerably more acidic ($pH_{25°C} = 2.2$) than the other Suzette fluids ($pH_{25°C} = 3.5$–3.7) and contains substantially higher concentrations of dissolved Fe, ΣH_2S, and Al. Although F is abundantly present in magmatic volatiles, its elevated concentration in the SZ5 fluids relative to the other Suzette fluids (Table 1) is not diagnostic of increased magmatic volatile input. Laboratory experiments and field observations have demonstrated that F is readily incorporated into hydrous secondary minerals and may be subsequently released to solution under changing temperature and pH conditions (Seyfried and Ding, 1995; Seewald et al., 2015), as is likely the case at SZ5.

The observed fluid chemistry at SZ5 is consistent with re-equilibration of the common source fluid with previously altered rock containing a aluminosilicates and iron sulfides mineral assemblage that is devoid of mobile trace elements such as Cs, Rb, and Li. Comparison of the NS6 fluid characterized by a $pH_{25°C}$ of 2.8 to nearby smoker fluids NS3 and NS5 with $pH_{25°C}$ values between 3 and 4, shows a similar compositional relationship, suggesting that all the North Su fluids are derived from a common source fluid, but NS6 has reacted with previously altered rocks. The coexistence of high and low $pH_{25°C}$ fluids at Suzette and North Su implies that spatial heterogeneity in the alteration of crustal rocks in hydrothermal upflow zones allows some deep-seated source fluids to reach the seafloor without encountering rocks previously altered by acid-sulfate fluids. Moreover, the model suggests that the lower $pH_{25°C}$ values of the SZ5 and NS6 fluids are an indirect result of previous episodes of magmatic degassing and fluid-rock interaction that altered the composition and mineralogy of the oceanic crust, and does not reflect the active entrainment of magmatic volatiles.

The EQ3NR/EQ6 computer code was used to test the hypothesis that the low pH SZ5 fluids at Suzette reflect re-equilibration of a less acidic seawater derived hydrothermal fluid ($pH_{25°C} = 3$–4) with rocks previously altered in hydrothermal upflow zones by acidic magmatic volatiles. For this model, the common source fluid was represented by the Mg- and ΣSO_4-free SZ1 fluid with an initial $pH_{25°C}$ of 3.7. The SZ1 fluid was incrementally reacted with a pyrophyllite-quartz-pyrite-alunite mineral assemblage at 272 °C (the inferred reaction zone temperature at SZ5 prior to mixing), 250 bar and a final water/rock mass ratio of 1 (Model #2, Table 2). Quartz and chalcedony formation were suppressed in the model to approximate aqueous SiO_2 concentrations in excess of quartz and chalcedony saturation as observed in the Suzette endmember fluids. The reaction path model produced a more acidic fluid characterized by a measured $pH_{25°C}$ of 2.0 (2.4 *in situ*) that was not substantially modified in terms of its major element composition (Table 2). The stable mineral assemblage after equilibration consists of pyrophyllite-cristobalite-pyrite-alunite-anhydrite. The model results demonstrate that reaction of an evolved hydrothermal fluid with a $pH_{25°C}$ of 3–4 with a secondary assemblage containing pyrophyllite-quartz-pyrite-alunite produces a fluid that is similar to the SZ5 fluid in terms of its composition and $pH_{25°C}$.

The higher $pH_{25°C}$ of the NS6 fluids (2.8) relative to SZ5 fluids (2.2) suggests buffering by a different secondary alteration assemblage that does not contain alunite (see Fig. 10). Reaction of an evolved moderately acidic common source fluid represented by the NS3 vent fluid ($pH_{25°C} = 3.4$) with a mineral assemblage containing pyrophyllite-quartz-pyrite mineral solution at 325 °C, 250 bar and a final water/rock mass ratio of 1, produced a mineral assemblage consisting of pyrophyllite-quartz-pyrite-muscovite(illite)-anhydrite and reproduced the NS6 fluid composition (Model #3, Table 2). Similar fluid temperatures, $pH_{25°C}$, and chemistry at South Su suggest that the same mineral assemblage may buffer fluid composition during upflow.

Collectively, results of the thermodynamic models demonstrate that low $pH_{25°C}$ values observed in many smoker fluids venting at the seafloor in back-arc environments do not reflect the direct addition of acidity by magmatic volatiles during convective circulation. Instead, the venting of low $pH_{25°C}$ smoker fluids may be the result of chemical re-equilibration with rocks altered previously by magmatic volatiles in hydrothermal upflow zones. Prior episodes of hydrothermal activity involving fumarolic venting of acid-sulfate fluids formed by the mixing of magmatic volatiles with seawater in subsurface environments (Seewald et al., 2015) are likely responsible for the formation of pyrophyllite and alunite bearing mineral assemblages in hydrothermal upflow zones. Thus, the acidity of magmatic volatiles may be "stored" in the oceanic crust through the creation of acid-sulfate mineral assemblages and subsequently released to seawater-derived smoker fluids that reoccupy permeable flow paths.

The reaction path models used to reproduce the SZ5 and NS6 fluid compositions demonstrated that the fluids equilibrate at water/rock mass ratios of 6 and 200, respectively, and did not undergo significant compositional change with continued reaction to the final water/rock ratio of 1. Constant fluid composition over this broad range of water/rock ratios demonstrates the high capacity of minerals to buffer fluid chemistry in subsurface environments. The ability of secondary alteration assemblages to lower the pH of smoker-type fluids at values below 3 will ultimately depend on the time integrated water/rock mass ratios in upflow zones. Because the pH buffering capacity in hydrothermal upflow zones will be exhausted at sufficiently high water/rock ratios, the lowering of $pH_{25°C}$ to values between 2 and 3 during upflow is likely a transient phenomenon.

5.4. Metal remobilization

The chemical interaction of previously altered regions of the oceanic lithosphere with smoker-type vent fluids during upflow has important implications for the mobilization of sulfide-forming metals in subseafloor environments. Interaction of a seawater-derived smoker fluids with quartz-illite-pyrophyllite-anhydrite ± alunite assemblages substantially increases acidity and the solubility of metal-bearing minerals, leading to dissolution in the upflow zone. Because Fe and Al have high concentrations in unaltered crustal rocks and are relatively immobile, they may persist in highly altered hydrothermal upflow zones, and contribute to vent fluid chemistry. For metals present in trace quantities, however, extensive alteration may rapidly exhaust the reservoir initially available in unaltered rock.

Some data suggest that acidic magmatic fluids released from shallow magma chambers may contain high levels of magma-derived metals that contribute to the formation seafloor mineral deposits (Yang and Scott, 1996, 2002, 2006; Heinrich, 2007; Heinrich and Candela, 2014). These same magmatic fluids are responsible for altering volcanic rocks to acid-sulfate mineral assemblages that may subsequently be responsible for the acidification of smoker fluids during upflow. Reaction of acidic magmatic volatiles with fresh crustal rocks will result in the titration of acidity and increased *in situ* pH. Increasing pH during rock alteration may induce precipitation of Fe, Cu, Zn, and Pb sulfide minerals in upflow zones which may be remobilized during subsequent acidification of seawater-derived smoker fluids during reaction with acid-sulfate mineral assemblages.

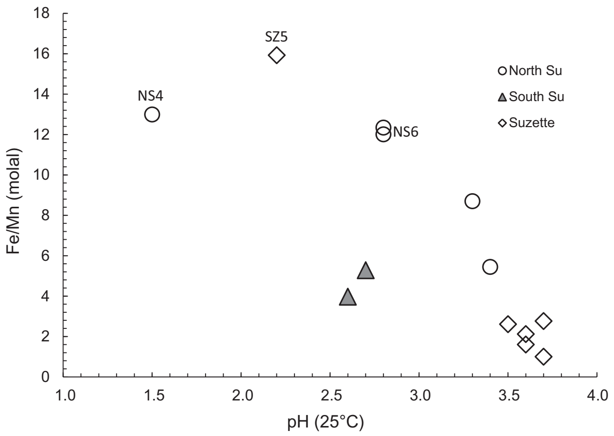

Fig. 12. Fe/Mn molal ratios versus $pH_{25°C}$ for hydrothermal fluids venting at SuSu Knolls.

Evidence for metal mobilization during acidification of smoker fluids at SuSu Knolls is provided by the relative abundances of dissolved Fe and Mn, which typically show similar responses to variations in H^+ activity in terms of their aqueous solubility (Seyfried, 1987; Seewald and Seyfried, 1990). Unaltered crustal rocks at SuSu Knolls contain <0.2 wt.% MnO while FeO_{total} values are as high as 7.25 wt.% (Beier et al., 2015). Due to the substantially lower abundance of Mn, it is expected that crustal rocks extensively altered by interaction with highly acidic magmatic fluids will be rapidly depleted in Mn, but contain substantial quantities of Fe. Due to the substantially greater abundance of Fe over Mn, observed systematic increases in Fe/Mn molal ratios with decreasing $pH_{25°C}$ within a given vent field at SuSu Knolls (Fig. 12) are consistent with extensive mobilization of Fe, but not Mn, during acidification of smoker fluids in upflow zones.

Because hydrothermal upflow zones previously altered by magmatic fluids may be highly enriched in magmatically-derived metals such as Cu, Zn, and Pb, smoker fluids may mobilize these metals by the same acidification process that produced elevated Fe concentrations. Thus, a portion of the dissolved metals present in black-smoker fluids may ultimately be derived from magmatic fluids, but require seawater-derived hydrothermal fluids for delivery to the seafloor.

6. SUMMARY AND CONCLUSIONS

The composition of seawater-derived hydrothermal fluids venting at the SuSu Knolls back-arc extensional environment indicates formation via a series of sequential fluid-rock reactions during convective circulation through the oceanic lithosphere. The chemistry of seawater is extensively modified during high temperature fluid-rock reactions at low water/rock mass ratios in deep-seated reaction zones to produce a moderately acidic fluid that is similar in composition to vent fluids observed at mid-ocean ridges ($pH_{25°C} \approx 3$–4). The composition of smoker fluids venting in back-arc environments, however, is characterized by a wider range of $pH_{25°C}$ that includes substantially more acidic values.

Equilibrium thermodynamic models demonstrate that mixing of magmatic fluids exsolved from active magma chambers may contribute acidic volatile species to back-arc smoker vent fluids, but cannot represent the source of acidity responsible for their lower $pH_{25°C}$ if the magmatic fluids are added prior to or during reaction with fresh crustal rocks. We postulate that higher acidity of some back-arc smoker vent fluids ($pH_{25°C} \approx 2$–3) reflects reaction in regions of the oceanic crust that have been previously altered by highly acidic magmatic fluids to an assemblage containing quartz-illite-pyrophyllite-anhydrite ± alunite. Chemical equilibration of seawater-derived smoker fluids with these highly altered assemblages generates substantial acidity that lowers pH and may result in the aqueous remobilization of magmatically-derived metals from hydrothermal upflow zones. At the seafloor, precipitation as sulfide minerals upon mixing with cold alkaline seawater may result in the formation of seafloor massive sulfide deposits. Such a model implies that the high acidity and metals released during the exsolution of magmatic fluids from silicic magmas may be stored in the oceanic crust and subsequently harvested by seawater-derived hydrothermal fluids.

Other geochemical processes also play an important role in regulating the composition of smoker fluids at SuSu Knolls. Some vent fluids are actively phase separating at the seafloor while others may undergo phase separation below the seafloor. Because the chlorinity of smoker fluids may be substantially enriched relative to seawater by leaching of Cl from felsic rocks, vapor phases produced during phase separation may be characterized by aqueous Cl concentrations in excess of seawater values. Hydrothermal interaction with hemipelagic sediments that are abundantly present at SuSu Knolls contributes significant quantities of thermogenically produced carbon species such as CH_4 to smoker vent fluids. Elevated Mg concentrations in many samples along with non-conservative behavior of SO_4 in response to anhydrite precipitation, provides evidence for subseafloor mixing of high temperature Mg- and SO_4-free endmember fluids with cold Mg- and SO_4-rich seawater.

Fumarolic venting of magmatic fluids in proximity to hydrothermal activity involving the convective circulation of seawater-derived smoker fluids at SuSu Knolls represents a powerful opportunity to constrain chemical and physical processes that regulate the composition of hydrothermal fluids in back-arc environments. Our results demonstrate that silicic magma chambers play a fundamental role in regulating vent fluid chemistry. Much of the compositional variability exhibited by hydrothermal fluids in back arc-environments reflects past or ongoing degassing of highly acidic magmatic volatiles. A deep understanding of these processes will play a fundamental role in the development of models to describe the impact of hydrothermal activity in arc and back-arc environments on the formation of seafloor massive sulfide deposits and global geochemical fluxes associated with subduction.

ACKNOWLEDGEMENTS

We thank the *Jason* group and the crew of the RV *Melville* for their expertise, assistance, and dedication that contributed to a very successful field program. The authors are very grateful to Janis Thal for assistance in generating the composite bathymetric map of the SuSu Knolls complex. This study received financial support from NSF Grant OCE-0327448, the WHOI Deep Ocean Exploration Institute Graduate Fellowship to E.P. Reeves, the Ocean Drilling Program Schlanger Fellowship to P.R. Craddock and a fellowship from the Hanse-Wissenschaftskolleg to J.S. Seewald.

APPENDIX A. SUPPLEMENTARY MATERIAL

Supplementary data to this article can be found online at https://doi.org/10.1016/j.gca.2019.03.034.

REFERENCES

Albarède F., Michard A., Minster J. F. and Michard G. (1981) $^{87}Sr/^{86}Sr$ ratios in hydrothermal waters and deposits from the East Pacific Rise at 21°N. *Earth Planet. Sci. Lett.* **55**, 229–236.

Alt J. C. (1995) Subseafloor processes in mid-ocean ridge hydrothermal systems. In *Seafloor Hydrothermal Systems: Physical, Chemical, Biological, and Geological Interactions, AGU Monograph*, 91 (eds. S. E. Humphris, R. A. Zierenberg, L. S. Mullineaux and R. E. Thomson). American Geophysical Union, pp. 85–114.

Auzende J. M., Hashimoto J., Fialamedioni A. and Ohta S. (1997) In situ geological and biological study of two hydrothermal zones in the Manus Basin (Papua New Guinea). *Comptes Rendus De L Academie Des Sciences Serie Ii Fascicule A-Sciences De La Terre Et Des Planetes* **325**(8), 585–591.

Auzende J. M., Ishibashi J., Beaudoin Y., Charlou J. L., Delteil J., Donval J. P., Fouquet Y., Gouillou J. P., Ildefonse B. and Kimura H., et al. (2000) The eastern and western tips of Manus Basin (Papua, New Guinea) explored by submersible; MANAUTE cruise. *Comptes Rendus De L Academie Des Sciences Serie Ii Fascicule A-Sciences De La Terre Et Des Planetes* **331**(2), 119–126.

Bach W., Roberts S., Vanko D. A., Binns R. A., Yeats C. J., Craddock P. R. and Humphris S. E. (2003) Controls of fluid chemistry and complexation on rare-earth element contents of anhydrite from the PACMANUS subseafloor hydrothermal system, Manus Basin, Papua New Guinea. *Miner. Deposita* **38**(8), 916–935.

Beier C., Bach W., Turner S., Niedermeier D., Woodhead J., Erzinger J. and Krumm S. (2015) Origin of silicic Magmas at spreading centres—an example from the South East Rift, Manus Basin. *J. Petrol.* **56**, 255–272.

Berndt M. E., Seyfried W. E. and Beck J. W. (1988) Hydrothermal alteration processes at midocean ridges: experimental and theoretical constraints from Ca and Sr exchange reactions and Sr isotopic ratios. *J. Geophys. Res.* **93**(B5), 4573–4583.

Berndt M. E., Seyfried W. E. and Janecky D. R. (1989) Plagioclase and epidote buffering of cation ratios in mid-ocean ridge hydrothermal fluids—experimental results in and near the supercritical region. *Geochim. Cosmochim. Acta* **53**(9), 2283–2300.

Binns R. A. and Scott S. D. (1993) Actively forming polymetallic sulfide deposits associated with felsic volcanic-rocks in the Eastern Manus Back-Arc Basin, Papua New Guinea. *Econ. Geol.* **88**(8), 2226–2236.

Binns R. A., Scott S. D., Gemmell J. B., Crook K. and Party S. S. (1997) The SuSu Knolls Hydrothermal Field, Eastern Manus Basin, Papua New Guinea. *EOS Trans. AGU* **78**(722), Fall Meet. Suppl. Abstract V22E-02.

Binns R. A., Barriga F. J. A. S. and Miller D. J. (2007) Leg 193 Synthesis: Anatomy of an active felsic-hosted hydrothermal system, Eastern Manus Basin, Papua New Guinea. In *Proceedings of the Ocean Drilling Program, Scientific Results*, 193 (eds. F. J. A. S. Barriga, R. A. Binns, D. J. Miller and P. M. Herzig), pp. 1–71.

Bischoff J. L. and Rosenbauer R. J. (1985) An emprical equation of state for hydrothermal seawater (3.2 percent NaCl). *Am. J. Sci.* **285**, 725–763.

Bischoff J. L. and Seyfried W. E. (1978) Hydrothermal chemistry of seawater from 25 to 350 °C. *Am. J. Sci.* **278**, 838–860.

Boschen R. E., Rowden A. A., Clark M. R. and Gardner J. P. A. (2013) Mining of deep-sea seafloor massive sulfides: A review of the deposits, their benthic communities, impacts from mining, regulatory frameworks and management strategies. *Ocean Coast. Manage.* **84**, 54–67.

Both R., Crook K., Taylor B., Brogan S., Chappell B., Frankel E., Liu L., Sinton J. and Tiffin D. (1986) Hydrothermal chimneys and associated fauna in the Manus back-arc basin, Papua New Guinea. *EOS Trans. AGU* **67**, 489–491.

Bowers T. S. and Taylor H. P. (1985) An integrated chemical and stable-isotope model of the origin of midocean ridge hot spring systems. *J. Geophys. Res.* **90**(B14), 12583–12606.

Butterfield D. A., Jonasson I. R., Massoth G. J., Feely R. A., Roe K. K., Embley R. E., Holden J. F., McDuff R. E., Lilley M. D. and Delaney J. R. (1997) Seafloor eruptions and evolution of hydrothermal fluid chemistry. *Philos. Trans. R. Soc. Lond. A: Math. Phys. Eng. Sci.* **355**(1723), 369–386.

Butterfield D. A. and Massoth G. J. (1994) Geochemistry of North Cleft Segment vent fluids—temporal changes in chlorinity and their possible relation to recent volcanism. *J. Geophys. Res.: Solid Earth* **99**(B3), 4951–4968.

Butterfield D. A., McDuff R. E., Mottl M. J., Lilley M. D., Lupton J. E. and Massoth G. J. (1994) Gradients in the composition of hydrothermal fluids from the Endeavour Segment vent field: phase separation and brine loss. *J. Geophys. Res.: Solid Earth* **99**(B5), 9561–9583.

Butterfield D. A., Nakamura K., Takano B., Lilley M. D., Lupton J. E., Resing J. A. and Roe K. K. (2011) High SO_2 flux, sulfur accumulation, and gas fractionation at an erupting submarine volcano. *Geology* **39**, 803–806.

Butterfield D., Seyfried W. E. and Lilley M. (2003) Composition and evolution of hydrothermal fluids. In *Dahlem Workshop Report: Energy and Mass Transfer in Marine Hydrothermal Systems*, 89 (eds. P. E. Halbach, V. Tunnicliffe and J. R. Hein). Dahlem University Press, pp. 123–161.

Campbell A. C., Palmer M. R., Klinkhammer G. P., Bowers T. S., Edmond J. M., Lawrence J. R., Casey J. F., Thompson G., Humphris S., Rona P. and Karson J. A. (1988) Chemistry of hot springs on the Mid-Atlantic Ridge. *Nature* **335**, 514–519.

Craddock P. R. (2008) *Geochemical tracers of processes affecting the formation of seafloor hydrothermal fluids and deposits in the Manus back-arc basin* Ph.D. thesis. MIT–WHOI Joint Program in Oceanography. MIT.

Craddock P. R., Bach W., Seewald J. S., Rouxel O. J., Reeves E. and Tivey M. K. (2010) Rare earth element abundances in hydrothermal fluids from the Manus Basin, Papua New Guinea: indicators of sub-seafloor hydrothermal processes in back-arc basins. *Geochim. Cosmochim. Acta* **74**, 5494–5513.

Craig H. and Gordon L. I. (1965) Deuterium and oxygen 18 variations in the ocean and marine atmosphere. In *Stable Isotopes in Oceanographic Studies and Paleotemperatures* (ed. E. Tongiogi). Consiglio Nazionale Delle Ricerche, Laboratorio Di Geologia Nucleare, Pisa, pp. 9–130.

Craig H. (1969) Abyssal carbon-13 in the South Pacific. *J. Geophys. Res.* **74**, 5491–5506.

Cruse A. M. and Seewald J. S. (2006) Geochemistry of low-molecular weight hydrocarbons in hydrothermal fluids from Middle Valley, northern Juan de Fuca Ridge. *Geochim. Cosmochim. Acta* **70**, 2073–2092.

Cruse A. M. and Seewald J. S. (2010) Low-Molecular Weight Hydrocarbons in Vent Fluids from the Main Endeavour Field, northern Juan de Fuca Ridge. *Geochim. Cosmochim. Acta* **74**, 6126–6140.

Cruse A. M., Seewald J. S., Saccocia P. J. and Zierenberg R. (2008) Hydrothermal fluid composition at Middle Valley, northern Juan de Fuca Ridge: temporal and spatial variability. In *AGU Monograph, Modeling Hydrothermal Processes at Oceanic Spreading Centers: Magma to Microbe* (eds. R. Lowell, J. Seewald, A. Metaxis and M. Perfit), pp. 145–166.

de Ronde C. E. J. (2011) Submarine hydrothermal activity and gold-rich mineralization at Brothers Volcano, Kermadec Arc, New Zealand. *Mineral. Deposita* **46**, 541–584.

de Ronde C. E. J., Hannington M. D., Stoffers P., Wright I. C., Ditchburn R. G., Reyes A. G., Baker E. T., Massoth G. J., Lupton J. E. and Walker S. L., et al. (2005) Evolution of a submarine magmatic-hydrothermal system: Brothers volcano, southern Kermadec arc, New Zealand. *Econ. Geol.* **100**(6), 1097–1133.

de Ronde C. E. J. and Stucker V. K. (2015) Seafloor hydrothermal venting at volcanic arcs and backarcs. In *The Encyclopedia of Volcanoes* (eds. H. Sigurdsson, B. Houghton, S. McNutt, H. Rymer and J. Stix), second ed. Elsevier Inc., pp. 823–849.

Douville E., Bienvenu P., Charlou J. L., Donval J. P., Fouquet Y., Appriou P. and Gamo T. (1999a) Yttrium and rare earth elements in fluids from various deep-sea hydrothermal systems. *Geochim. Cosmochim. Acta* **63**(5), 627–643.

Douville E., Charlou J. L., Donval J. P., Hureau D. and Appriou P. (1999b) As and Sb behaviour in fluids from various deep-sea hydrothermal systems. *Comptes Rendus de L'Academie des Sciences Serie Ii Fascicule A-Sciences de La Terre et des Planetes* **328**(2), 97–104.

Drummond S. E. (1981) *Boiling and mixing of hydrothermal fluids: chemical effects on mineral precipitation* Ph.D. Dissertation. Penn. State University.

Eickmann B., Bach W., Rosner M. and Peckmann J. (2009) Geochemical constraints on the modes of carbonate precipitation in peridotites from the Logatchev Hydrothermal Vent Field and Gakkel Ridge. *Chem. Geol.* **268**(1–2), 97–106.

Fouquet Y., Vonstackelberg U., Charlou J. L., Erzinger J., Herzig P. M., Muhe R. and Wiedicke M. (1993) Metallogenesis in back-arc environments – The Lau Basin example. *Econ. Geol.* **88**(8), 2154–2181.

Gamo T., Sakai H., Ishibashi J., Nakayama E., Isshiki K., Matsuura H., Shitashima K., Takeuchi K. and Ohta S. (1993) Hydrothermal plumes in the Eastern Manus Basin, Bismarck Sea - CH_4, Mn, Al and pH anomalies. *Deep-Sea Res. Part I-Oceanogr. Res. Pap.* **40**(11–12), 2335–2349.

Gamo T., Okamura K., Charlou J. L., Urabe T., Auzende J. M., Ishibashi J., Shitashima K. and Chiba H. (1997) Acidic and sulfate-rich hydrothermal fluids from the Manus back-arc basin, Papua New Guinea. *Geology* **25**(2), 139–142.

Gamo T., Ishibashi J., Tsunogai U., Okamura K. and Chiba H. (2006) Unique geochemistry of submarine hydrothermal fluids from arc-back-arc settings of the Western Pacific. In *Back-Arc Spreading Systems: Geological, Biological, Chemical, and Physical Interactions. AGU Monograph*, 166 (eds. D. M. Christie, C. R. Fisher, S.-M. Lee and S. Givens). American Geophysical Union, pp. 147–161.

Gena K., Mizuta T., Ishiyama D. and Urabe T. (2001) Acid-sulphate type alteration and mineralization in the DESMOS caldera, Manus back-arc basin, Papua New Guinea. *Resour. Geol.* **51**, 31–44.

Gena K. R., Chiba H., Mizuta T. and Matsubaya O. (2006) Hydrogen, oxygen and sulfur isotope studies of seafloor hydrothermal system at the Desmos caldera, Manus back-arc basin, Papua New Guinea: an analogue of terrestrial acid hot crater-lake. *Resour. Geol.* **56**, 183–190.

German C. R. and Seyfried, Jr, W. E. (2014) Hydrothermal Processes. In *Treatise on Geochemistry* (eds. H. D. Holland and K. K. Turekian), second ed. Elsevier, Oxford, pp. 191–233.

Giggenbach W. F. (1992) Isotopic shifts in waters from geothermal and volcanic systems along convergent plate boundaries and their origin. *Earth Planet. Sci. Lett.* **113**, 495–510.

Hedenquist J. W. and Lowenstern J. B. (1994) The role of magmas in the formation of hydrothermal ore deposits. *Nature* **370**, 519–527.

Heinrich C. A. (2007) Fluid-fluid interactions in magmatic-hydrothermal ore formation. *Rev. Mineral. Geochem.* **65**, 363–387.

Heinrich C. A. and Candela (2014) Fluids and ore formation in the earth's crust. In *Treatise on Geochemistry, 2nd ed., Vol. 13: Geochemistry of Mineral Deposits* (eds. H. Holland and K. Turekian). Elsevier, pp. 1–28.

Helgeson H. C., Delany J. M., Nesbitt H. W. and Bird D. K. (1978) Summary and critique of the thermodynamic properties of rock-forming minerals. *Amer. J. Sci.* **278A**, 1–229.

Holland H. D. (1965) Some applications of thermochemical data to problems in ore deposits II. Mineral assemblages and the composition of ore-forming fluids. *Econ. Geol.* **60**, 1101–1166.

Holland H. D. and Malinin S. D. (1979) The solubility and occurrence of non-ore minerals. In *Geochemistry of Hydrothermal Ore Deposits* (ed. H. L. Barnes). Wiley, pp. 461–508.

Hrischeva E., Scott S. D. and Weston R. (2007) Metalliferous sediments associated with presently forming volcanogenic massive sulfides: The SuSu knolls hydrothermal field, eastern manus basin, Papua New Guinea. *Econ. Geol.* **102**(1), 55–73.

Ishibashi J., Wakita K., Okamura K., Gamo T., Shitashima K., Charlou J. L., Donval J. P., Jean-Baptiste P. and Party A. T. S. S. (1996) Chemical characteristics of hydrothermal fluids from the Manus back-arc basin, Papua New Guinea, II. Gas Components. *EOS Trans. AGU* **77**(W116), WPGM Suppl. Abstract T32A-6.

Iwasaki I. and Ozawa T. (1960) Genesis of sulfate in acid hot spring. *Bull. Chem. Soc. Jpn.* **33**, 1018–1019.

Johnson J. W., Oelkers E. H. and Helgeson H. C. (1992) SUPCRT92: a software package for calculating the standard molal thermodynamic properties of minerals, gases, aqueous species, and reactions from 1 to 5000 bar and 0 to 1000 °C. *Comput. Geosci.* **18**, 899–947.

Javoy M., Pineau F. and Iiyama J. T. (1978) Experimental determination of the isotopic fractionation between gaseous CO_2 and carbon dissolved in the tholeiitic magma: a preliminary study. *Contrib. Mineral. Petrol.* **67**, 35–39.

Kamenetsky V. S., Binns R. A., Gemmell J. B., Crawford A. J., Mernagh T. P., Maas R. and Steele D. (2001) Parental basaltic melts and fluids in eastern Manus backarc Basin: implications for hydrothermal mineralisation. *Earth Planet. Sci. Lett.* **184**, 685–702.

Kawagucci S., Chiba H., Ishibashi J.-I., Yamanaka T., Toki T., Muramatsu Y., Ueno Y., Makabe A., Inoue K., Yoshida N., Nakagawa S., Nunoura T., Takai K., Takahata N., Sano Y., Narita T., Teranishi G., Obata H. and Gamo T. (2011) Hydrothermal fluid geochecmistry at the Iheya North field in the mid-Okinawa Trough: Implications for origin of methane in subseafloor curculation systems. *Geochem. J.* **45**, 109–124.

Kawagucci S., Ueno Y., Takai K., Toki T., Ito M., Inoue K., Makabe A., Yoshida N., Muramatsu Y., Takahata N., Sano Y., Narita Y., Teranishi G., Obata H., Nakagawa S., Nunoura T. and Gamo T. (2013) Geochemical origin of hydrothermal fluid methane in sedimentassociated fields and its relevance to the geographical distribution of whole hydrothermal circulation. *Chem. Geol.* **339**, 213–225.

Kelley D. S. (1996) Methane-rich fluids in the oceanic crust. *J. Geophys. Res.* **101**, 2943–2962.

Kelley D. S. and Früh-Green G. L. (1999) Abiogenic methane in deep-seated mid-ocean ridge environments: Insights from stable isotope analyses. *J. Geophys. Res.* **104**, 10439–10460.

Kendall C. and Coplen T. B. (1985) Multisample conversion of water to hydrogen by zinc for stable isotope determination. *Anal. Chem.* **57**(7), 1437–1440.

Kusakabe M., Komoda Y., Takano B. and Abiko T. (2000) Sulfur isotopic effects in the disproportionation reaction of sulfur dioxide in hydrothermal fluids: implications for the δ34S variations of dissolved bisulfate and elemental sulfur from active crater lakes. *J. Volcanol. Geotherm. Res.* **97**, 287–307.

Lackschewitz K. S., Devey C. W., Stoffers P., Botz R., Eisenhauer A., Kummetz M., Schmidt M. and Singer A. (2004) Mineralogical, geochemical and isotopic characteristics of hydrothermal alteration processes in the active, submarine, felsic-hosted PACMANUS field, Manus Basin, Papua New Guinea. *Geochim. Cosmochim. Acta* **68**(21), 4405–4427.

Lee S. M. and Ruellan E. (2006) Tectonic and magmatic evolution of the Bismarck Sea, Papua New Guinea: review and new synthesis. In *Back-Arc Spreading Systems: Geological, Biological, Chemical, and Physical Interactions, AGU Monograph*, vol. 166 (eds. D. M. Christie, C. R. Fisher, S.-M. Lee and S. Givens). American Geophysical Union, pp. 263–286.

Lilley M. D., Butterfield D. A., Olson E. J., Lupton J. E., Macko S. A. and McDuff R. E. (1993) Anomalous CH_4 and NH_4^+ concentrations at an unsedimented mid-ocean-ridge hydrothermal system. *Nature* **364**, 45–47.

Lisitsyn A. P., Crook K., Bogdanov Y. A., Zonenshain L. P., Murav'yev K. G., Tufar W., Gurvich Y. G., Gordeyev V. V. and Ivanov G. V. (1993) A hydrothermal field in the rift zone of the Manus Basin, Bismarck Sea. *Int. Geol. Rev.* **35**(2), 105–126.

Martinez F. and Taylor B. (1996) Backarc spreading, rifting, and microplate rotation, between transform faults in the Manus basin. *Mar. Geophys. Res.* **18**(2–4), 203–224.

Mattey D. P. (1991) Carbon dioxide solubility and carbon isotope fractionation in basaltic melt. *Geochim. Cosmochim. Acta* **55** (11), 3467–3473.

McCollom T. M. and Seewald J. S. (2007) Abiotic synthesis of organic compounds in deep-sea hydrothermal environments. *Chem. Rev.* **107**, 382–401.

McDermott J. M., Seewald J. S., German C. R. and Sylva S. P. (2015) Pathways for abiotic organic synthesis at submarine hydrothermal fields. *Proc. Nat. Acad. Sci.* **112**, 7668–7672.

Moss R. and Scott S. D. (2001) Geochemistry and mineralogy of gold-rich hydrothermal precipitates from the eastern Manus Basin, Papua New Guinea. *Can. Mineral.* **39**, 957–978.

Mottl M. J., Seewald J. S., Wheat C. G., Tivey M. K., Michael P. J., Proskurowski G., McCollom T. M., Reeves E., Sharkey J., You C. F., Chan L. H. and Pichler T. (2011) Chemistry of hot springs along the Eastern Lau Spreading Center. *Geochim. Cosmochim. Acta* **75**, 1013–1038.

Park S. H., Lee S.-M., Kamenov G. D., Kwon S.-T. and Lee K.-Y. (2010) Tracing the origin of subduction components beneath the South East rift in the Manus Basin, Papua New Guinea. *Chem. Geol.* **269**, 339–349.

Pearce J. A. and Stern R. J. (2006) Origin of back-arc basin magmas: trace element and isotope perspectives. In *Back-Arc*

Spreading Systems: Geological, Biological, Chemical, and Physical Interactions. AGU Monograph (eds. D. M. Christie, C. R. Fisher, S.-. M. Lee and S. Givens). American Geophysical Union, pp. 63–86.

Pester N. J., Reeves E. P., Rough M. E., Ding K., Seewald J. S. and Seyfried, Jr., W. E. (2012) Subseafloor phase equilibria in high-temperature hydrothermal fluids of the Lucky Strike Seamount (Mid-Atlantic Ridge, 37°17'N). *Geochim. Cosmochim. Acta* **90**, 303–322.

Proskurowski G., Lilley M. D., Seewald J. S., Olson E. J., Früh-Green G. L., Lupton J. E., Sylva S. P. and Kelley D. S. (2008) Abiogenic hydrogen and hydrocarbon production at the lost city hydrothermal field. *Science* **319**, 604–607.

Redfield A. C. and Friedman I. (1965) Factors affecting the distribution of deuterium in the ocean. In *Symposium on Marine Geochemistry* (eds. D. R. Schink and J. T. Corliss). Occasional Publication No. 3. Narragansett Marine Laboratory, University of Rhode Island, pp. 149–168.

Rees C. E., Jenkins W. J. and Monster J. (1978) Sulfur isotopic composition of ocean water sulfate. *Geochim. Cosmochim. Acta* **42**, 377–381.

Reeves E. P., Seewald J. S., Saccocia P., Bach W., Craddock P. R., Shanks W. C., Sylva S. P., Walsh E., Pichler T. and Rosner M. (2011) Geochemistry of hydrothermal fluids from the PACMANUS, Northeast Pual and Vienna Woods hydrothermal fields, Manus Basin, Papua New Guinea. *Geochim. Cosmochim. Acta* **75**, 1088–1123.

Resing J. A., Lebon G., Baker E. T., Lupton J. E., Embley R. W., Massoth G. J., Chadwick W. W. and De Ronde C. E. J. (2007) Venting of acid-sulfate fluids in a high-sulfidation setting at NW Rota-1 submarine volcano on the Mariana Arc. *Econ. Geol.* **102**, 1047–1061.

Resing J. A., Baker E. T., Lupton J. E., Walker S. L., Butterfield D. A., Massoth G. J. and Nakamura K. (2009) Chemistry of hydrothermal plumes above submarine volcanoes of the Mariana Arc. *G-Cubed* **10**. https://doi.org/10.1029/2008GC002141.

Roberts S., Bach W., Binns R. A., Vanko D. A., Yeats C. J., Teagle D. A. H., Blacklock K., Blusztajn J. S., Boyce A. J. and Cooper M. J., et al. (2003) Contrasting evolution of hydrothermal fluids in the PACMANUS system, Manus Basin: the Sr and S isotope evidence. *Geology* **31**(9), 805–808.

Scaillet B. and Pichavant M. (2003) Experimental constraints on volatile abundances in arc magmas and their implications for degassing processes. *Geol. Soc., Lond., Spec. Publ.* **213**, 23–52.

Schoell M. (1988) Multiple origins of methane in the Earth. *Chem. Geol.* **71**, 1–10.

Seewald J., Cruse A. and Saccocia P. (2003) Aqueous volatiles in hydrothermal fluids from the Main Endeavour Field, northern Juan de Fuca Ridge: temporal variability following earthquake activity. *Earth Planet. Sci. Lett.* **216**(4), 575–590.

Seewald J. S., Doherty K. W., Hammar T. R. and Liberatore S. P. (2002) A new gas-tight isobaric sampler for hydrothermal fluids. *Deep-Sea Res. Part I-Oceanogr. Res. Pap.* **49**(1), 189–196.

Seewald J. S., Reeves E. P., Bach W., Saccocia P. J., Craddock P. R., Shanks, III, W. C., Sylva S. P., Pichler T., Rosner M. and Walsh E. (2015) Submarine venting of magmatic volatiles in the Eastern Manus Basin, Papua New Guinea. *Geochim. Cosmoshim. Acta* **163**, 178–199.

Seewald J. S. and Seyfried, Jr., W. E. (1990) The effect of temperature on heavy and base metal mobility in subseafloor hydrothermal systems: constraints from basalt alteration experiments and field studies. *Earth Planet. Sci. Lett.* **101**, 388–403.

Seewald J. S., Seyfried, Jr., W. E. and Shanks, III, W. C. (1994) Variations in the chemical and stable isotope composition of carbon and sulfur species during organic-rich sediment alteration: an experimental and theoretical study of hydrothermal activity at Guaymas Basin, Gulf of California. *Geochim. Cosmochim. Acta* **58**, 5065–5082.

Seewald J. S., Seyfried, Jr., W. E. and Thornton E. C. (1990) Organic-rich sediment alteration: an experimental and theoretical study at elevated temperatures and pressures. *Appl. Geochem.* **5**, 193–209.

Seyfried W. E. (1987) Experimental and theoretical constraints on hydrothermal alteration processes at mid-ocean ridges. *Ann. Rev. Earth Planet. Sci.* **15**, 317–335.

Seyfried W. E. and Ding K. (1995) The hydrothermal chemistry of fluoride in seawater. *Geochimic. Cosmochim. Acta* **59**, 1063–1071.

Seyfried W. E., Ding K. and Berndt M. E. (1991) Phase equilibria constraints on the chemistry of hot spring fluids at mid-ocean ridges. *Geochim. Cosmochim. Acta* **55**, 3559–3580.

Seyfried W. E., Janecky D. R. and Mottl M. J. (1984) Alteration of the oceanic crust: implications for geochemical cycles of lithium and boron. *Geochim. Cosmochim. Acta* **48**(3), 557–569.

Shanks, III, W. C., Böhlke J. K. and Seal R. R. (1995) Stable isotopes in mid-ocean ridge hydrothermal systems: interactions between fluids, minerals, and organisms. In *Seafloor Hydrothermal Systems: Physical, Chemical, Biological, and Geological Interactions. AGU Monograph*, 91 (eds. S. E. Humphris, R. A. Zierenberg, L. S. Mullineaux and R. E. Thomson). American Geophysical Union, pp. 194–221.

Shanks, III, W. C. (2001) Stable isotopes in seafloor hydrothermal systems: vent fluids, hydrothermal deposits, hydrothermal alteration, and microbial processes. *Rev. Mineral. Geochem.* **43**, 469–525.

Shock E. L. and Helgeson H. C. (1988) Calculation of the thermodynamic and transport properties of aqueous species at high pressures and temperatures: correlation algorithms for ionic species and equation of state predictions to 5 kb and 1000 °C. *Geochim. Cosmochim. Acta* **52**, 2009–2036.

Shock E. L., Helgeson H. C. and Sverjensky D. A. (1989) Calculation of the thermodynamic and transport properties of aqueous species at high pressures and temperatures: standard partial molal properties of inorganic neutral species. *Geochim. Cosmochim. Acta* **53**, 2157–2183.

Shock E. L., Sassani D. C., Willis M. and Sverjensky D. A. (1997) Inorganic species in geologic fluids: correlations among standard molal thermodynamic properties of aqueous ions and hydroxide complexes. *Geochim. Cosmochim. Acta* **61**, 907–950.

Sinton J. M., Ford L. L., Chappell B. and McCulloch M. T. (2003) Magma genesis and mantle heterogeneity in the Manus back-arc basin, Papua New Guinea. *J. Petrol.* **44**, 159–195.

Spencer D. W., Robertson D. E., Turekian K. K. and Folsom T. R. (1970) Trace element calibrations and profiles at the GEOSECS test station in the Northeast Pacific Ocean. *J. Geophys. Res.* **75** (36), 7688–7696.

Sverjensky D. A., Shock E. L. and Helgeson H. C. (1997) Prediction of the thermodynamic properties of aqueous metal complexes to 1000 °C and 5 kb. *Geochim. Cosmochim. Acta.* **61**, 1359–1412.

Tagirov B. and Schott J. (2001) Aluminum speciation in crustal fluids revisited. *Geochim. Cosmochim. Acta* **65**, 3965–3992.

Takai K., Nunoura T., Ishibashi J. I., Lupton J., Suzuki R., Hamasaki H., Ueno Y., Kawagucci S., Gamo T. and Suzuki Y., et al. (2008) Variability in the microbial communities and hydrothermal fluid chemistry at the newly discovered Mariner hydrothermal field, southern Lau Basin. *J. Geophys. Res. – Biogeosci.* **113**(G02031). https://doi.org/10.1029/2007JG000636.

Taylor B. (1979) Bismarck Sea: evolution of a back-arc basin. *Geology* **7**(171–174).

Taylor B., Crook K. and Sinton J. (1994) Extensional transform zones and oblique spreading centers. *J. Geophys. Res.-Solid Earth* **99**(B10), 19707–19718.

Thal J., Tivey M., Yoerger D. R. and Bach W. (2016) Subaqueous cryptodome eruption, hydrothermal activity and related seafloor morphologies on the andesitic North Su volcano. *J. Volcanol. Geotherm. Res.* **323**, 80–96.

Thal J., Tivey M., Yoerger D., Jöns N. and Bach W. (2014) Geologic setting of PACManus hydrothermal area – high resolution mapping and in situ observations. *Mar. Geol.* **355**, 98–114.

Thode H. G. and Monster J. (1965) Sulfur-isotope geochemistry of petroleum, evaporites, and ancient seas. In *Fluids in Subsurface Environments: A Symposium*, v. 4 (eds. A. Young and J. E. Galley). Am. Assoc. Petroleum Geologists Mem., pp. 367–377.

Tivey M., Bach W., Seewald J. S., Tivey M. K., Vanko D. A. and Shipboard Science Party (2006) *Cruise Report for R/V Melville Cruise MGLN06MV—Hydrothermal Systems in the Eastern Manus Basin: Fluid Chemistry and Magnetic Structure as Guides to Subseafloor Processes*. Woods Hole Oceanographic Institution http://hdl.handle.net/1912/4077.

Tregoning P. (2002) Plate kinematics in the western Pacific derived from geodetic observations. *J. Geophys. Res.-Solid Earth* **107** (B1).

Tufar W. (1990) Modern hydrothermal activity, formation of complex massive sulfide deposits and associated vent communities in the Manus Back-arc Basin (Bismarck Sea, Papua New Guinea). *Mitteilung der Osterreichen Geologischen Gesellshaft* **82**, 183–210.

Van Driessche A. E. S., Canals A., Ossorio M., Reyes R. C. and García-Ruiz J. M. (2016) Unraveling the sulfate sources of (giant) gypsum crystals using gypsum isotope fractionation factors. *J. Geol.* **124**, 235–245.

Von Damm K. L. (1995) Controls on the chemistry and temporal variability of seafloor hydrothermal systems. In *Seafloor Hydrothermal Systems: Physical, Chemical, Biological, and Geological Interactions. AGU Monograph*, 91 (eds. S. E. Humphris, R. A. Zierenberg, L. S. Mullineaux and R. E. Thomson). American Geophysical Union, pp. 222–247.

Von Damm K. L. (2004) Evolution of the hydrothermal system at East Pacific Rise 9°50'N: geochemical evidence for changes in the upper oceanic crust. In *Mid-Ocean Ridges: Hydrothermal Interactions Between the Lithosphere and Oceans. Geophys. Monogr. Ser.*, 148 (eds. C. R. German, J. Lin and L. M. Parson). AGU, Washington, DC, pp. 285–305.

Von Damm K. L. and Bischoff J. L. (1987) Chemistry of hydrothermal solutions from the Southern Juan De Fuca Ridge. *J. Geophys. Res.: Solid Earth Planet* **92**(B11), 11334–11346.

Von Damm K. L., Bray A. M., Buttermore L. G. and Oosting S. E. (1998) The geochemical controls on vent fluids from the Lucky Strike vent field, Mid-Atlantic Ridge. *Earth Planet. Sci. Lett.* **160**(3–4), 521–536.

Von Damm K. L., Buttermore L. G., Oosting S. E., Bray A. M., Fornari D. J., Lilley M. D. and Shanks W. C. (1997) Direct observation of the evolution of a seafloor 'blank smoker' from vapour to brine. *Earth Planet. Sci. Lett.* **149**(1–4), 101–111.

Von Damm K. L., Edmond J. M., Grant B. and Measures C. I. (1985a) Chemistry of submarine hydrothermal solutions at 21° N, East Pacific Rise. *Geochim. Cosmochim. Acta* **49**(11), 2197–2220.

Von Damm K. L., Edmond J. M., Measures C. I. and Grant B. (1985b) Chemistry of submarine hydrothermal solutions at Guaymas Basin, Gulf of California. *Geochim. Cosmochim. Acta* **49**, 2221–2237.

Von Damm K. L., Lilley M. D., Shanks W. C., Brockington M., Bray A. M., O'Grady K. M., Olson E., Graham A., Proskurowski G. and The SouEPR Science Party (2003) Extraordinary phase separation and segregation in vent fluids from the southern East Pacific Rise. *Earth Planet. Sci. Lett.* **206**, 365–378.

Von Damm K. L., Parker C. M., Zierenberg R. A., Lilley M. D., Olson E. J., Clague D. A. and Mcclain J. S. (2005) The Escanaba Trough, Gorda Ridge hydrothermal system: temporal stability and subseafloor complexity. *Geochim. Cosmochim. Acta* **69**(21), 4971–4984.

Von Damm K. L., Parker C. M., Lilley M. D., Olson E. J., Clague D. A., Zierenberg R. A. and McClain J. S. (2006) Chemistry of vent fluids and its implications for subsurface conditions at Sea Cliff hydrothermal field, Gorda Ridge. *G-Cuberd* **71**. https://doi.org/10.1029/2005GC001034.

Wang D. T., Reeves E. P., McDermott J. M., Seewald J. S. and Ono S. (2018) Clumped isotopologue constraints on the origin of methane at seafloor hot springs. *Geochim. Cosmochim. Acta* **223**, 141–158.

Welhan J. A. (1988) Origins of methane in hydrothermal systems. *Chem. Geol.* **71**(1–3), 183–198.

Welhan J. A. and Lupton J. E. (1987) Light hydrocarbon gases in Guaymas Basin hydrothermal fluids: thermogenic versus abiogenic origin. *Bull. Am. Assoc. Pet. Geol.* **71**, 215–223.

Whiticar M. J. (1999) Carbon and hydrogen isotope systematics of bacterial formation and oxidation of methane. *Chem. Geol.* **161**, 291–314.

Whiticar M. J., Faber E., Whelan J. K. and Simoneit B. R. T. (1994) Thermogenic and bacterial hydrocarbon gases (free and sorbed) in Middle Valley, Juan de Fuca Ridge, Leg 139. In *Proc. ODP, Sci. Results*, 139 (eds. M. J. Mottl, E. E. Davis, A. T. Fisher and J. F. Slack), pp. 467–477.

Wolery T. J. (1992) *EQ3NR, A Computer Program for Aqueous Speciation-Solubility Calculations: Theoretical Manual, Users's Guide, and related Documentation*. Lawrence Livermore National Lab.

Wolery T. J. and Daveler S. A. (1992) *EQ3NR, A Computer Program for Aqueous Speciation-Solubility Calculations: Theoretical Manual, Users's Guide, and related Documentation*. Lawrence Livermore National Lab.

Yang K. H. and Scott S. D. (1996) Possible contribution of a metal-rich magmatic fluid to a sea-floor hydrothermal system. *Nature* **383**, 420–423.

Yang K. H. and Scott S. D. (2002) Magmatic degassing of volatiles and ore metals into a hydrothermal system on the modern sea floor of the eastern Manus back-arc basin, western Pacific. *Econ. Geol.* **97**, 1079–1100.

Yang K. H. and Scott S. D. (2006) Magmatic fluids as a source of metals in seafloor hydrothermal systems. In *Back-Arc Spreading Systems: Geological, Biological, Chemical, and Physical Interactions, AGU Monograph* (eds. D. M. Christie, C. R. Fisher, S.-. M. Lee and S. Givens). American Geophysical Union, pp. 163–184.

Yeats C. J., Parr J. M., Binns R. A., Gemmell J. B. and Scott S. D. (2014) The SuSu Knolls hydrothermal field, eastern Manus Basin, Papua New Guinea: an active submarine high-sulfidation copper-gold system. *Econ. Geol.* **109**(8), 2207–2226.